HHS Public Access

Author manuscript

Mol Psychiatry. Author manuscript; available in PMC 2022 December 01.

Published in final edited form as:

Mol Psychiatry. 2022 August ; 27(8): 3272–3285. doi:10.1038/s41380-022-01557-z.

Brain-Specific Deletion of GIT1 Impairs Cognition and Alters Phosphorylation of Synaptic Protein Networks Implicated in Schizophrenia Susceptibility

Daniel M. Fass[1,2,*], **Michael C. Lewis**[1,6,*], **Rushdy Ahmad**[4,7,*], **Matthew J. Szucs**[4,8], **Qiangge Zhang**[3], **Morgan Fleishman**[1,3], **Dongqing Wang**[3], **Myung Jong Kim**[1,9], **Jonathan Biag**[1,10], **Steven A. Carr**[4], **Edward M. Scolnick**[1,4], **Richard T. Premont**[5], **Stephen J. Haggarty**[1,2]

[1]Stanley Center for Psychiatric Research, Broad Institute of MIT and Harvard, 75 Ames Street, Cambridge, Massachusetts 02142, USA

[2]Chemical Neurobiology Laboratory, Center for Genomic Medicine, Departments of Neurology & Psychiatry, Massachusetts General Hospital, Harvard Medical School, Boston, Massachusetts 02114, USA

[3]McGovern Institute for Brain Research, Department of Brain and Cognitive Sciences, Massachusetts Institute of Technology, Cambridge, MA 02139, USA

[4]Broad Institute of MIT and Harvard, 415 Main Street, Cambridge, MA, 02142, USA

[5]Harrington Discovery Institute, Cleveland, OH, 44106, USA; Institute for Transformative Molecular Medicine, Case Western Reserve University, Cleveland, OH, 44106, USA

[6]Sage Therapeutics, Cambridge, MA, USA

[7]Wyss Institute at Harvard University, Boston, MA, USA

[8]Department of Biochemistry and Molecular Genetics, University of Colorado Denver School of Medicine, Aurora, Colorado, USA

[9]Department of Neurology, Northwestern University Feinberg School of Medicine, Chicago, Illinois, USA

[10]Novartis Pharmaceuticals, Cambridge, MA, USA

Abstract

Correspondence: Dr. Stephen J. Haggarty (shaggarty@mgh.harvard.edu).

*Equal contribution.

Author Contributions

SJH, EMS, DMF, MCL, RA, MJK, RTP, and SAC designed the study. DMF, MCL, MJS, QZ, MF, DW, JB, RTP, and SJH conducted the experiments and analyzed data. DMF and SJH wrote the manuscript, and all authors edited the manuscript.

Conflict of Interest

S. J. Haggarty is a member of the SAB and equity holder of Psy Therapeutics, Frequency Therapeutics, Sensorium Therapeutics, 4M Therapeutics, and Proximity Therapeutics; and has received speaking/consulting fees from AstraZeneca, Amgen, Merck, and Syros, and RBNC. D.M. Fass has received consulting fees from Psy Therapeutics. None of these entities were involved in the current study.

Despite tremendous effort, the molecular and cellular basis of cognitive deficits in schizophrenia remain poorly understood. Recent progress in elucidating the genetic architecture of schizophrenia has highlighted the association of multiple loci and rare variants that may impact susceptibility. One key example, given their potential etiopathogenic and therapeutic relevance, is a set of genes that encode proteins that regulate excitatory glutamatergic synapses in brain. A critical next step is to delineate specifically how such genetic variation impacts synaptic plasticity and to determine if and how the encoded proteins interact biochemically with one another to control cognitive function in a convergent manner. Towards this goal, here we study the roles of GPCR-kinase interacting protein 1 (GIT1), a synaptic scaffolding and signaling protein with damaging coding variants found in schizophrenia patients, as well as copy number variants found in patients with neurodevelopmental disorders. We generated conditional neural-selective *GIT1* knockout mice and found that these mice have deficits in fear conditioning memory recall and spatial memory, as well as reduced cortical neuron dendritic spine density. Using global quantitative phospho-proteomics, we revealed that GIT1 deletion in brain perturbs specific networks of GIT1-interacting synaptic proteins. Importantly, several schizophrenia and neurodevelopmental disorder risk genes are present within these networks. We propose that GIT1 regulates the phosphorylation of a network of synaptic proteins and other critical regulators of neuroplasticity, and that perturbation of these networks may contribute specifically to cognitive deficits observed in schizophrenia and neurodevelopmental disorders.

Introduction

Neuropsychiatric disorders are devastating illnesses affecting brain function that cause tremendous suffering in patients and families worldwide. Intellectual disability neurodevelopmental (ID/NDD) disorders, with an overall prevalence of ~1%, comprise a heterogeneous group of largely monogenic disorders that feature severe cognitive deficits either alone or in combination with syndromes of effects across other body systems[1]. Schizophrenia (SCZ), with a lifetime prevalence of ~0.7%[2], features positive symptoms (hallucinations, delusions), negative symptoms (flat affect, avolition), and cognitive deficits[3, 4]. While ID/NDD and SCZ are clearly distinct disorders (e.g. ID/NDD is typically found in young children, while SCZ typically first presents in late adolescence/early adulthood), the shared domain of cognitive deficits suggests some convergent dysfunction.

Recent large-scale exome sequencing and genome-wide association efforts have yielded tremendous progress in identifying the genetic risk factors for neuropsychiatric diseases. For ID/NDD, over 700 risk genes have been identified[1]. Common and rare variants contributing to schizophrenia (SCZ) risk have been identified at over 100 genomic loci[5–9]. In comparisons of the cell biological functions of ID/NDD and SCZ risk genes, a number of common themes emerge[10, 11], which may reflect the commonality of cognitive deficits across these disorders. In particular, numerous ID/NDD and SCZ risk genes play key roles within pre-synaptic and post-synaptic specializations in neurons in the central nervous system. On the pre-synaptic side, studies suggest dysregulation of presynaptic vesicle recruitment, docking, release, and recycling in both ID/NDD (e.g.[12, 13]) and schizophrenia[14]. Post-synaptically, many ID/NDD and SCZ risk genes regulate glutamate

receptor signaling[15], as well as the dendritic spine actin cytoskeleton via effects on RHO GTPase and CAMKII signaling[1, 16]. Thus, the synapse is a hot spot for neuropsychiatric disease risk gene pathology.

Here we investigated GIT1, a synaptic signaling and scaffolding protein (reviewed in [17]). We propose that GIT1 plays central roles in synaptic neuropsychiatric disease risk gene pathology. Rare coding variants in *GIT1* are found in schizophrenia patients[6, 7]. Several of these schizophrenia-associated coding variants disrupt GIT1 activation of the p21-activated kinase PAK3[18], a kinase with expression levels that are dysregulated in the brains of schizophrenia patients[19]. Recently, a splice acceptor site variant in *GIT1* was found in a schizophrenia patient[8]. In addition, copy number variation at the *GIT1* locus, including both deletions and duplications, has been reported in patients with ID/NDD[20]. The fact that *GIT1* is a loss of function intolerant gene[21] strengthens the notion that these variants are pathological. Lastly, GIT1 has been reported to physically interact or form complexes with the schizophrenia risk gene products CNKSR2 ([5, 22]; CNSKR2 is also an ID risk gene—[23]), PTPRF[5, 24], and GRIA1[5, 24], as well as the ID/NDD risk gene products ARHGEF6[25, 26] and PAK3 [26, 27], all of which can be found at the synapse or at post-synaptic dendritic spines[28–30]. These data strongly support the notion that GIT1 is a key protein that may regulate the function of multiple neuropsychiatric disease risk genes that may be involved in cognitive function.

GIT1 has been reported to function on both the pre-synaptic and post-synaptic sides of synapses (reviewed in [17]). In pre-synaptic terminals, GIT1 binds to the active zone cytomatrix protein PCLO[31]. Functionally, presynaptic GIT1 regulates the probability of vesicle release[32]. On the post-synaptic side, GIT1 facilitates targeting of AMPA receptors to the post-synaptic density and the synaptic membrane[24]. In addition, GIT1 plays key roles in dendritic spine formation and morphology[28] by interacting with a number of proteins that regulate the actin cytoskeleton in spines, such as RAC1 and PAK3[29]. With these multiple pre- and post-synaptic roles, GIT1 is a central regulator of synaptic transmission.

Given the key roles of GIT1 on both sides of synapses, involving interactions with ID/NDD and SCZ risk gene products, it is perhaps not surprising that *GIT1* loss of function in knockout mice causes cognitive deficits, such as decreased fear conditioning learning[33], an absence of novel object recognition and reduced spatial learning and memory in the Morris water maze test[34, 35], and impaired performance during operant learning[36]. However, all previous studies in *GIT1* loss of function mice involved whole body knockout; these mice suffer from substantial post-natal lethality[33] as well as impaired lung development[37]. Thus, it is unclear whether cognitive deficits observed in whole-body GIT1 knockout mice are due to abnormal brain function versus general functional impairment due to pulmonary insufficiency.

Here we use conditional neural-specific *GIT1* knockout (NKO) mice to investigate cognitive deficits due to loss of function of *GIT1* in the nervous system. Unlike whole-body *GIT1* knockout, conditional neural-specific *GIT1* knockout does not cause post-natal lethality. We find that these mice have deficits in both fear conditioning learning and working memory.

We then utilize a proteomic approach to analyze hippocampi from *GIT1*-NKO mice to identify protein phosphorylation events that depend on the presence of GIT1. We discuss the relevance of our findings for GIT1 regulation of protein networks involved in synaptic functions, and dysregulation of these networks and functions in neuropsychiatric diseases.

Materials and Methods

GIT1 Conditional Neural Knockout Mice

Floxed *Git1* mice[33] (Jackson Laboratories Mouse Genome Informatics symbol $Git1^{tm1.1Rtp}$) and Nestin-Cre (B6.Cg-Tg (Nes-cre)1Kln/J) mice were generously provided by Dr. Guoping Feng (MIT). Floxed *Git1* mice used here had been extensively (> 10 generations) backcrossed with C57BL/6 mice. Nestin-Cre mice were initially purchased from Jackson Laboratories (stock number 003771; genetic strain is the F2 hybrid of the closely related substrains C57BL/6 and C57BL/10) and then backcrossed with C57BL/6 mice. For breeding conditional *GIT1* neural-specific knockout mice according to the established protocol required to prevent germline transmission of the Nestin-Cre transgene[38], male $Git1^{flox/+}$, Cre^{+} transgenic mice were mated with female $Git1^{flox/flox}$ Cre^{-} mice to generate both neural knockout (GIT1-NKO; $Git1^{flox/flox}$ Cre^{+}) and control ($Git1^{flox/flox}$ Cre^{-}) males for behavioral testing. For some experiments (see below), Nestin-Cre mice were purchased from Jackson Laboratories for use as additional controls in behavior experiments. Genotyping was carried out under standard conditions utilizing a previously published protocol[33].

Behavioral studies—Mice were group housed (4/cage) in a temperature and humidity controlled room and maintained on a reverse 12:12 light/dark cycle (7:00 am-7:00 pm) with *ad libitum* access to food and water. All behavior assays used male mice aged 8–12 weeks, and were performed during the light period under low level white light illumination. Experimental procedures were approved by the MIT institutional animal care and use committee under protocol 1012–102-15.

All behavioral studies were carried out with experimenter blinded to genotype, and without randomization of animal testing order. The last cage bedding change occurred ~24 hours prior to the beginning of behavior testing. For all assays, mice were habituated in the test facility in their home cages for 1 hour prior to starting the task. Cohort 1 was tested in the following behavioral tests in a series: T-maze, 3-chamber social interaction, elevated plus maze, pre-pulse inhibition, and fear conditioning with at least four days between each behavioral experiment. We typically see no difference in responses when tests are run serially versus individually, with the critical exception that a test featuring a strong stressor, such as a footshock, can affect subsequent test responses. The only test with a strong stressor used here is fear conditioning, and thus fear conditioning was run as the last test. Follow up cohort 2 was run in T-maze and fear conditioning only as these demonstrated differences between control and *GIT1*-NKO mice in the initial cohort. Statistical tests for all behavior assays were conducted on data pooled from both cohorts which comprised a minimum of 8 to a maximum of 29 animals per group (see legend for Figure 1 for details) which met or

exceeded the number of animals required for sampling to achieve adequate power calculated as described in Dell et al., 2002.

T maze spontaneous alternation—The T maze spontaneous alternation test was run according to the procedure reported by Wolf and colleagues[39]. In this procedure, consecutive entry into all (3) arms not entered on the previous 2 trials was defined as correct alternation. Mice were placed in the start arm of the T-maze (5 cm wide x 28 cm long x 10 cm high; Stoelting) and allowed to freely explore the maze for 5 minutes; all arm entries were recorded. Chance performance in this task is 22%. Because we did not impose any delay between arm choices, performance on this test likely depends primarily on cortical activity[40].

Three-chamber social interaction—Male mice were used across all cohorts. Both stranger 1 and stranger 2 were wild type male S129 Sv males (Jackson laboratory) with matched age and body weight to test mice. Stranger mice were habituated by placing them inside an inverted wire cup for 30 minutes, two sessions per day for three consecutive days before experiments. Each stranger mouse was used maximally two times per day. The social test apparatus was made of a clear plexiglass box (65 (L) × 44 (W) × 30 (H) cm) with removable floor and partitions dividing the box into left, center, and right chambers. Center chamber (21 cm x 22 cm) is half the width of the left (21 cm x 44 cm) and right chamber (21 cm x 44 cm). These three chambers were interconnected with 5 cm openings between each chamber which can be closed or opened manually with a lever operated door. The inverted wire cups to contain the stranger mice were cylindrical, 10 cm in height, a bottom diameter of 10 cm with the metal bars spaced 0.8 cm apart. A weighted cup was placed on top of the inverted wire cups to prevent the test mice from climbing onto the wire cup. Each wire cup was used only one time per day then followed by extensive clean with 75% ethanol and water at the end of the test day. During the habituation phase, an empty wire cup was placed into left and right chamber, and the test mouse was placed into the middle chamber and allowed to explore for 15 minutes, with the doors into both side chambers open. During the sociability test phase, the test mouse was firstly gently introduced to the middle chamber with the doors to both side chambers closed, and an unfamiliar mouse (S1) was placed under the inverted wire cup in one of the side-chambers and a toy object (O) was placed under the inverted wire cup placed on the opposite side chamber. The location of the stranger mouse and object was counterbalanced between test trials to exclude side preference. The experimenter then lifted up the doorways to both side chambers simultaneously, and the test mouse was allowed to explore all three chambers for 15 minutes. During the social novelty test phase, the test mouse was again gently introduced into the middle chamber with the doors to both side chambers closed. Then a novel mouse (S2) was placed under the inverted wire cup, replacing the toy object (O) in one of the side-chambers. The experimenter then lifted up the doorways to both side chambers simultaneously, and the test mouse was allowed to explore all three chambers for an additional 15 minutes. Time spent in close proximity to the stranger mice or toy object was analyzed using Noldus Ethovison software.

Elevated plus maze—Mice were placed in a closed arm of an elevated plus maze (Arm width = 10 cm, arm length = 50 cm, wall height = 30 cm, distance from floor = 55 cm;

Coulbourn Instruments) and allowed to freely explore the maze for 5 minutes. Total time in the open and closed arms and the total distance travelled was recorded automatically via video tracking software (EthoVision).

Acoustic startle response and prepulse inhibition—Each test chamber was equipped with a loudspeaker mounted 25 cm above the holding cylinder and a commercial startle reflex system (SR Lab, San Diego Instruments, CA). Individual mouse was placed inside the plexiglass holding cylinder mounted on a plexiglass platform. A piezoelectric accelerometer located beneath the platform was used to transform startle responses into units based on force and latency of startle. Data were collected at 250 samples/s and the maximum voltage attained on each trial was used as the dependent variable. Each test session started with a 5 minute acclimation period in the presence of 65 dB acoustic background noise followed by five 120 dB startle pulses. Pre-pulse trials followed the initial 120 dB startle acclimation. Each pre-pulse stimulation was 20 ms in duration, followed by a 40 ms startle stimulus of 120 dB. PPI was recorded for pre-pulse intensities of 70, 75, 80, 85 and 90 dB, and no stimulus. Each prepulse trial was administered ten times in a random order. Trials of 120 dB alone were randomly interspersed within the pre-pulse trials and used for comparison with the prepulse trials. The percent PPI was calculated using the formula [100−(response to pre-pulse + 120 dB)/(response for 120 dB alone)×100]. Acoustic startle trials were followed the PPI trials. Startle trials consisted of 40 ms pulses at 0 (no stimulus), 70, 75, 80, 85, 90, 95, 100, 105, 110, 115, and 120 dB. Each trial was presented five times in a randomized order.

Fear Conditioning

Fear conditioning assays were run according to the procedures reported by Loftipour and colleagues[41]. These procedures utilize two tone-shock pairings for fear conditioning learning; we reasoned that two tone-shock pairings should be sufficient for learning because whole-body GIT1 knockout mice have fear conditioning deficits that are evident with even a single tone-shock pairing[33].

Training: Mice were placed in one of two fear conditioning chambers (Coulbourn Instruments) and allowed to freely explore for 2 minutes (baseline). After 2 minutes, mice were presented with a 30s white noise (85dB) conditioned stimulus (CS) with a co-terminating 2s foot shock (0.75mA; US). Freezing was measured continuously for 2 minutes after the first CS-US presentation (immediate) which also served as the inter-trial interval (ITI). Mice were then presented with a second 30s CS co-terminating 2s US pairing, followed by 30s before being removed from the training chamber. All freezing behavior was automatically scored by Freeze Frame software (Coulbourn) defined as a complete absence of movement other than respiration for a full second.

Context Test: 24 hours after initial training, mice were placed back into the original training chamber and freezing was measured continuously for 5 minutes (context).

Cued Test: One hour after contextual testing, the chambers were altered (grid floor covered with a smooth plastic floor (tactile); wall cues added (visual); vanilla extract scent added

(olfactory)) and freezing was measured for 2 ½ minutes (Pre-CS). Then, the 85dB white noise was presented and freezing was measured continuously for 2 ½ minutes (cued).

Behavioral Data Analysis

All behavioral data were collected by automated methods to remove potential confounds associated with human scoring, with the exception of spontaneous alternation in the T-maze, which was scored by the experimenter in real time, blinded to genotype. T-tests or repeated measures analysis of variance (ANOVA) were utilized where appropriate. All data were analyzed via SPSS v. 24

Golgi-Cox Staining and Dendritic Spine Quantitation

Brains were rapidly harvested from 4 WT and 4 GIT1-NKO mice following cervical dislocation and immediately placed in impregnation solution (FD Rapid GolgiStain kit, FD Neurotechnologies catalog # PK-401) for two weeks. After 1 week in Golgi C solution, the brains were rapidly frozen in isopentane/dry ice. 200-μm thick coronal sections were cut using a Zeiss sliding microtome chilled with dry ice, and sections were air dried on gelatin-subbed slides and then stained using the manufacturer's recommended procedures. Mid-layer cortical neurons were imaged with a 40X oil immersion objective on a Zeiss LSM 800 Airyscan confocal microscope at the Massachusetts General Hospital Program in Membrane Biology Microscopy Core facility (https://researchcores.partners.org/pmb/about). Dendrite fragments chosen for analysis were branches emerging from apical dendrites. Z-stacks of images were acquired (0.5 μm interval between images in the z-axis) to allow capture of dendrite fragments > 20 μm in length. Images were analyzed using ZEN software (Zeiss). Z-stacks were collapsed using the ZEN Extended Depth of Focus function (variance mode), and dendrite lengths were determined by tracing with the Spline Curve function. Spines with typical structures as defined in Hering & Sheng (2001) occurring along the dendrites were counted by hand by an experimenter who was blind to genotype. In total, ~2.5 mm of dendrite lengths were analyzed per genotype. Dendritic spine densities were compared in WT and GIT1-NKO mice by an unpaired, two-tailed T-test using GraphPad Prism software. Upon visual inspection, there was no obvious change in spine morphology induced by *GIT1* knockout, as has been reported previously[42], though further study involving 3D reconstruction of dendritic spines would be necessary to confirm this in a quantitative manner.

Total and Phospho-proteomics

Total hippocampal proteins and phospho-proteins were detected by quantitative LC-MS/MS methods. Mass spectrometry detection and quantitation was performed in quadruplicate with paired samples consisting of male, 8–12 week old matched pairs (either littermates or age-matched) of control and GIT1-NKO mice. Following decapitation, mice heads were dipped in liquid nitrogen for 5 seconds to rapidly cool, but not freeze, the brain. Hippocampi were dissected rapidly on a cooling tray, and placed in Covaris bags (tissueTUBE TT05, Covaris), which were then flash frozen in liquid nitrogen. The frozen tissue was pulverized according to the manufacturer's protocol on a Covaris CP02 Cryoprep Pulverizer. The pulverized tissue was lysed in 8M urea with protease and phosphatase inhibitors. The protein lysate (typical total yield ~1–1.5 mg per hippocampus) was reduced, alkylated, and double

digested with both Lys-C and Trypsin overnight. Equivalent amounts of tryptic peptides (~1 mg) from each sample were labeled with TMT-10 reagent (Thermo Fisher Scientific) and the individual label incorporation was checked via LC-MS/MS. All samples had greater than 95% label incorporation. The labeled digests were combined and fractionated using basic reverse phase (bRP) chromatography (with an Agilent HPLC system) into 2 fractions for proteome analysis and 12 fractions for phosphopeptide analysis. Fractionation decreases sample complexity and increases the dynamic range of detection. From each fraction, 5% of the total volume was used for proteomic analysis while the remaining 95% was used for phosphopeptide enrichment using established protocol for Immobilized Metal Affinity Chromatography (IMAC) developed at the Broad Institute[43, 44]. The proteome and the phosphoproteome data were acquired on a Q-Exactive+ mass spectrometer (Thermo Fisher Scientific). The original mass spectra and the protein sequence database used for searches have been deposited in the public proteomics repository MassIVE (http://massive.ucsd.edu) and are accessible at ftp://massive.ucsd.edu/MSV000089025/. Peptide spectrum matching and protein identification was performed using Spectrum Mill (Agilent). Peptide identification false discovery rates (FDRs) were calculated at 3 different levels: spectrum, distinct peptide, and distinct protein. Peptide FDRs were calculated in SM using essentially the same pseudo-reversal strategy evaluated by Elias and Gygi[45] and shown to perform the same as library concatenation. A false distinct protein ID occurs when all the distinct peptides that group together to constitute a distinct protein have a deltaForwardReverseScore ≤ 0. We adjusted settings to provide peptide FDR of 1–2% and protein FDR of 0–1%. SM also carries out sophisticated protein grouping using the methods previously described[46]. Only proteins with >2 peptides and at least 2 TMT ratios in each replicate are counted as being identified and quantified. For each matched pair of control and *GIT1*-NKO hippocampi, Spectrum Mill calculated a fold-change for each protein or phospho-site (psite). Our initial criterion for a GIT1-regulated 'hit' was a requirement that fold-changes from all four matched sample pairs had to be coherent, i.e. in the same direction (up or down). We then normalized the mean of these four psite fold changes to the mean of the fold changes of the corresponding proteins induced by GIT1 neural knockout. For quantitating protein levels and fold changes, only peptides unique to individual proteins were counted; thus, peptides that are identical across multiple gene homologs were not counted. We then ranked our normalized psite fold change list by the magnitude of the change induced by GIT1 neural knockout. Lastly, we imposed a minimum fold change threshold of 25% (up or down); the 639 phospho-protein changes meeting these criteria are shown in Supplemental Table 7.

GO category enrichment analyses—GO category enrichment analysis for all detected hippocampal proteins (Figure 2B) and GIT1-regulated phospho-proteins (Figure 3B) was performed using the Enrichment Analysis (PANTHER) web tool at www.geneontology.org, which output both fold-enrichment values and corrected false discovery rate p values (Supplemental Table 2). To generate the treemaps in Figures 2B and 3B, we started with the indicated sets of enriched cellular component GO categories with corrected p values < $1e^{-05}$. We removed GO categories that could not be linked to a specific cellular component (e.g. "Cell" and "Intracellular"), and then we manually annotated each remaining GO category to its corresponding specific cellular component (e.g. the GO category "Chromatin"

was annotated as being in the “Nucleus” component). Our manually annotated cellular components were the branches (shown as distinct colors on the treemap; branch names are shown as white text in each branch) of the treemap, with enriched GO categories as the leaves (individual lettered boxes in each branch). Leaf size was determined by the fold-enrichment value for each GO category. GO cellular component category enrichment among GIT1-regulated phospho-peptides (Supplemental Figure 3; Supplemental Table 7) was also quantitated and visualized with the BiNGO plugin[47] in Cytoscape version 3.5.1. The BiNGO visualization shows the GO cellular component categories as circular ‘nodes’ that were found to be statistically significantly enriched, superimposed on the corresponding regions of the GO hierarchy. Node size is proportional to the number mouse hippocampal phospho-peptides (Supplemental File 1) of GIT1-regulated phospho-protein (Supplemental Figure 3) genes that are annotated to that node’s GO cellular component category. Node color reflects the corrected p-value for enrichment: white nodes are not significantly enriched; colored nodes have significant p-values ranging from yellow (p between 0.001–$1E^{-7}$) to dark orange ($p < 1E^{-7}$).

Molecular interaction and function enrichment database search—Molecular interaction and function (i.e. biological pathway) enrichment was performed using the expert curated biological pathway web tool Reactome (www.reactome.org). Using the ‘Analyze Data’ function, mouse protein sets (see Results) were entered, converted to human equivalents, and evaluated for pathway over-representation using default settings.

GIT1 proximity labeling Bio-ID protein interaction screen

A lentiviral construct was generated to express a fusion protein consisting of the promiscuous biotinylase BirA fused to the C-terminus of GIT1 (Supplemental Figure 4). Lentiviral infection introduced this construct into human neural progenitor cells (NPCs) and Neurogenin-2 differentiated neurons according to methods described in[48]. After incubation of cells in the presence of 50 μM exogenous biotin for 18 hrs, we used streptavidin beads to precipitate biotinylated proteins from GIT1-BirA expressing NPC or neurons (one large batch of cells grown in 15 cm plates for each cell type), and also from naive cells as a negative control, as described[49]. Mass spectrometric protein identification was performed at the Taplin Biological Mass Spectrometry Facility (https://taplin.med.harvard.edu/home) using an LTQ Orbitrap Velos Pro ion-trap mass spectrometer (Thermo Fisher Scientific, Waltham, MA). Streptavidin bead precipitate tryptic peptides were detected, isolated, and fragmented to produce a tandem mass spectrum of specific fragment ions for each peptide. Peptide sequences (and hence protein identity) were determined by matching protein databases with the acquired fragmentation pattern by the software program, Sequest (Thermo Fisher Scientific, Waltham, MA). All databases include a reversed version of all the sequences and the data was filtered to between a one and two percent peptide false discovery rate. We defined GIT1 interacting ‘hits’ as proteins purified by the streptavidin beads from GIT1-BirA expressing NPCs or neurons that were completely absent from naive cell streptavidin bead precipitates.

Results

Cognitive deficits in neural-specific conditional *GIT1* knockout mice

To analyze the behavioral consequences of GIT1 dysfunction in the context of intact neural circuits *in vivo*, we utilized a *GIT1* knockout mouse. Three distinct alleles generating whole-body *GIT1* knockout mice have been created, and mice with these knockout alleles have several learning and memory deficits[33, 34, 36]. However, whole-body *GIT1* knockout mice also have greatly reduced postnatal survival[33, 34] as well as cardiac, pulmonary, and skeletal dysfunction[36, 37, 50], potentially confounding the interpretation of behavioral data in these mice. To overcome these previous limitations and create a model system to investigate the neural-specific functions of GIT1, we utilized a conditional knockout approach by crossing Nestin-Cre expressing driver mice with one of the previously generated mouse strains carrying floxed *GIT1* alleles[33] to specifically inactivate *GIT1* in the central and peripheral nervous systems (*GIT1*-NKO mice; Figure 1A; Supplemental Figure 1). Analysis of adult hippocampal tissue from these neural-specific *GIT1*-NKO mice showed almost undetectable expression of GIT1 (Supplemental Figure 1). These mice had normal post-natal survival rates in contrast to the previously reported whole-body *GIT1* knockout mice, but were slightly smaller in overall body size similar to whole-body *GIT1* knockout mice (data not shown). Also similar to whole-body *GIT1* knockout mice, *GIT1*-NKO mice had lower cortical neuron dendritic spine density (Figure 1G and see Martyn et al., 2018), indicating that GIT1 function in the nervous system is required to support normal numbers of dendritic spines, and suggesting that *GIT1*-NKO mice might exhibit reduced cognitive function.

To broadly assess the behavioral consequences of neural-specific loss of GIT1, *GIT1*-NKO mice were put through a battery of tests. To assess cognition, *GIT1*-NKO mice were first tested in both contextual fear conditioning, which assesses a memory process dependent on both the hippocampus and the amygdala[51, 52], and cued fear conditioning, which assesses amygdala-dependent memory processes[52]. Figure 1B shows that *GIT1*-NKO mice exhibit both hippocampus- and amygdala-dependent fear conditioning deficits when compared to Nestin-Cre expressing, non-floxed $GIT1^{+/+}$ control mice. This did not simply reflect a difference in locomotor activity levels, as *GIT1*-NKO mice had no difference in freezing responses during the training period as compared to control mice ($p = 0.1315$; two-tailed t-test). Next, the mice were tested in a spontaneous alternation cortex--dependent working memory T-maze task[53, 54]. Figure 1C shows that *GIT1*-NKO mice had virtually no ability to recall arm visits in the T-maze, suggesting a severe working memory deficit. In contrast, *GIT1*-NKO mice had no deficits in social interaction (Figure 1E, three-chamber social interaction test, reviewed in [55]) or prepulse inhibition (Figure 1F), a test of sensorimotor gating, which is defective in schizophrenia patients (e.g. [56]). In addition, *GIT1*-NKO mice scored equivalent to control mice in the elevated plus maze test (Figure 1D), indicating that these mice have normal levels of anxiety. These results demonstrate that GIT1 function is critical specifically for cognitive learning and memory processes, and are in accordance with deficits in contextual and cued fear conditioning reported previously for whole-body *GIT1* knockout mice. Further, these results suggest that GIT1 dysfunction might contribute to impaired cognition, but not social or sensorimotor deficits, in schizophrenia patients.

Proteome-wide identification of GIT1-regulated phosphorylation events in hippocampus

GIT1 regulation of synaptic processes might occur simply by scaffolding to facilitate the proximal localization of key synaptic machinery components required for function. However, given the ability of GIT1 to regulate multiple kinase signaling cascades[17], GIT1 may also modulate synaptic processes by controlling the phosphorylation states of key synaptic proteins. To address this question in an unbiased manner, we employed mass spectrometry-based proteomics to discover GIT1-regulated phosphorylation events in mouse hippocampus. Notably, this analysis was proteome-wide—i.e. not restricted to synaptic proteins—as we used whole hippocampal lysate as the input into the proteomic pipeline. To preserve protein phosphorylation states in the hippocampi, mouse heads were quickly chilled after decapitation by a brief dip in liquid nitrogen[57]. Following dissection on a surface kept at −20 degrees, hippocampi were flash frozen in liquid nitrogen and then put through a standardized lysis process optimized for phospho-proteomics ([43, 44]; and see methods). Hippocampal lysates from wild-type and *GIT1*-NKO mice (four biological replicates of each) were then subjected to immobilized metal affinity chromatography enrichment-based phospho-peptide mass spectrometry detection and quantitation, as well as parallel proteomic detection and quantitation of total protein levels (Figure 2A).

To our knowledge, these proteomic data represent the most comprehensive survey to date of proteins and phospho-proteins expressed in the hippocampus (Figure 2A). We found that 8726 genes expressed at least one characterized protein product; these genes comprise nearly 40% of the protein coding genes in the mouse genome according to Gencode (http://www.gencodegenes.org/mouse_stats.html) (Supplemental Table 1). Confirming an expected expression pattern, these proteins include receptors for the major neurotransmitter systems that have been described in the hippocampus: glutamate, GABA, acetylcholine, dopamine, serotonin, and norepinephrine (Supplemental Table 1; [58, 59]). Gene ontology (GO) cellular component category enrichment analysis (using PANTHER; Figure 2B and Supplemental Table 2) showed the expected over-representation of proteins involved in synapses and neurites, and also highlighted the important roles of the nucleus, mitochondria, and the cytoskeleton, as well as other cellular components, in cells of the hippocampus. Similar GO category enrichment analyses for biological process and molecular functions are shown in Supplemental Table 2 Interestingly, our data support the notion of a role for the hippocampus in schizophrenia pathology[60]; of the 58 single-gene GWAS loci containing variants associated with schizophrenia risk identified by Ripke and colleagues[5], 36 of these express proteins we detected in the hippocampus (Supplemental Table 6). Lastly, as a key control, our proteomic data showed the expected large decrease in GIT1 levels in the neural knockout mice' hippocampi (Figure 2C; remaining residual levels of GIT1 are likely from vasculature). In addition, the GIT1-associated PIX proteins (ARHGEF6 and ARHGEF7) are downregulated by GIT1-NKO; this lack of stability of PIX proteins in the absence of GITs has been observed previously[17, 34]. GIT2 (both long and short isoforms) was observed to be upregulated potentially as compensation for the loss of GIT1 protein (Supplemental Figure 1). However, this apparent compensatory upregulation of GIT2 was unable to replace GIT1's role in cognitive behaviors (Figure 1), supporting the contention that GIT1 and GIT2 have different roles in the synapse[32]. These data underscore the variety and complexity of protein expression and function in the hippocampus.

While it is well-appreciated that regulation of protein phosphorylation is a key aspect of synaptic plasticity[61], our data also indicate the staggering complexity of protein phosphorylation in the hippocampus, with 29,623 unique phospho-peptides detected on 6596 proteins, many of which had multiple phosphorylation sites/states (Supplemental Table 3). By cross-referencing these phospho-peptides with published lists of synaptic proteins[30, 62], we can deduce that, at synapses, there may be up to 800 and 7526 distinct phospho-peptides (many synaptic proteins contain multiple phospho-peptides) on the pre- and post-synaptic sides, respectively (Figure 2D). Searching for these phosphorylation states in the PhosphoSite public protein post-translational modification database (www.phosphosite.org) revealed both known and previously unreported phosphorylation events, reflective of the depth of the proteomic analysis performed. For example, 14 phosphorylation sites were detected in GIT1, and all of those are present in the PhosphoSite database (Supplemental Table 4). In contrast, 35 phosphorylation sites were detected in the schizophrenia risk gene product GRIN2A, and 7 of those were apparently novel (i.e. not present in the PhosphoSite database; Supplemental Table 4). Global analysis of Gene Ontology (GO) cellular component category enrichment in the total set of all phospho-proteins in our data (Supplemental Table 3) using the BiNGO app in Cytoscape (http://www.cytoscape.org/) revealed 275 enriched ($p < 0.01$) GO categories, comprising many basic and neuron-specific cellular components (Supplemental Table 5; hierarchical network visualization in Supplemental File 1).

Parallel proteomic detection and quantitation of total protein levels allowed for normalization of phospho-peptide levels to the corresponding levels of total protein in wild-type and *GIT1*-NKO samples; these normalized phospho-peptide levels were then used to quantitate phosphorylation state changes induced by *GIT1* knockout. Our initial criteria for a 'hit' in this assay were: 1) a *GIT1* knockout-induced change in phosphorylation state in the same direction (up or down) across all four of our paired replicate samples; and 2) a minimum change up or down of 25%. A total of 639 protein phosphorylation state changes, of at least 25% up or down, were observed consistently across all samples (Supplemental Table 7; see Methods section for details of quantitation method).

Some of the proteins with phosphorylation states altered by *GIT1* knockout are known to directly interact or associate with GIT1, including ARHGEF6[17], GIT2[31], PCLO[31], CNKSR2[22], CAMK2A and CAMK2B[50], PTK2[63], MYO18A[64], PPFIA2[24], RIMS1[65], NCK1[66], and ERC2[67]; or to associate with ARHGEF6/7, including PAK1 and PAK2[26], SHANK1[68], and NSF[69]. Indeed, we have replicated several of these reported interactions with GIT1 (Supplemental Figure 2). The GIT1 interactor NCK1 also interacts with the kinase TNIK[70], and TNIK phosphorylates serine 315 in CAMK2B[71]; serine 315 phosphorylation was upregulated by *GIT1* knockout, suggesting that the GIT1-NCK1 interaction may inhibit TNIK. Supporting this notion, phosphorylation of a δ-catenin serine targeted by TNIK (serine 528 in CTNND2[71]) was also slightly upregulated by *GIT1* knockout (by ~16%, which was less than the 25% threshold we set for 'hits'; data not shown). Taken together, these data indicate that phosphorylation states of proteins may be regulated via their interactions with the GIT1-ARHGEF6/7 complex and kinases that are regulated by this complex.

Because GIT1 stimulates the activity of p21-activated kinases (PAKs) and microtubule-associated kinase (MAPK)[18], and GIT1 has been reported to scaffold MEK-ERK MAP kinases[72–74], and *GIT1* knockout indeed caused a decrease in phosphorylation of MEK1 at a serine residue targeted by PAK1 (Coles & Shaw, 2002; Supplemental Figure 5D), we anticipated that *GIT1* knockout would decrease the phosphorylation of known PAK and/or MAPK targets. Indeed, the phospho-site that was the most downregulated by *GIT1* knockout, serine 92 on SEPT3, may be a PAK target, as PAKs phosphorylate septins in yeast[75]. In addition, another one of the strongest effects of *GIT1* knockout was a decrease in phosphorylation of the microtubule destabilizer STMN1 at serine 63; this serine is known to be a target of PAK[76]. Likewise, *GIT1* knockout also decreases the phosphorylation of ARHGEF2, ARHGDIA, and SPEN, which are known targets of PAK[77–79]. Phosphorylation of PAK1 serine 144 and PAK2 serine 141, which get autophosphorylated upon PAK1/2 binding to GIT1/PIX (e.g. [18]), were downregulated by *GIT1* knockout. MYO18A phosphorylation was also decreased by *GIT1* knockout; MYO18A is a known PAK interactor[64]. Lastly, several other sites of phosphorylation decreased by GIT1 knockout (such as NSF serine 207, NSMF serine 72, DIRAS2 serine 35, and SCN1A serine 607) match, or nearly match, key characteristics of optimal PAK phospho-acceptor sites (R at position −2 and large hydrophobic residues—W, I, V, Y—at +1 to +2 relative to the phosphorylated serine[80]; these phospho-sites are highlighted in Supplemental Table 7). In addition, the phosphorylation of numerous KSP motifs in neurofilament H was decreased by *GIT1* knockout; these motifs can be phosphorylated by MAPK[81]. Thus, known GIT1 interactions and/or PAK/MAPK targets account for a subset of the GIT1-regulated phosphorylation state changes observed here; for the remainder, mechanisms of regulation are unknown, and these may represent previously undiscovered targets of PAKs, MAPKs, or other kinases.

Conditional neural *GIT1* knockout also induced substantial increases in the phosphorylation states of a number of proteins (Supplemental Table 7). We reasoned that this effect might be mediated by decreases in GIT1-regulated phosphatase activity. Indeed, there was a trend towards a decrease in protein phosphatase 2A catalytic subunit (PPP2CA) expression in GIT1 knockout hippocampi in our proteomics data (Supplemental Table 12), and we confirmed this as a statistically significant effect by western blotting analysis (Supplemental Figure 5). One of the proteins with increased phosphorylation in GIT1-NKO hippocampi is AGAP2, which is a known target of PP2A (Kubiniok et al., 2018). PP2A is known to interact with PAK3 in the brain (Westphal et al., 1999), and thus GIT1 may regulate PP2A via activation of PAK3. PP2A downregulation may underlie some of the cognitive deficits in *GIT1*-NKO mice, as PP2A catalytic subunit mutations in humans cause syndromic intellectual disability (Reynhout et al., 2019).

Biological network enrichment analysis of GIT1-regulated phospho-proteins

We detected 73 protein phosphorylation states that were robustly regulated (more than 2-fold) by *GIT1* knockout: 45 were downregulated, and 28 were upregulated (Figure 3A). We tested whether synaptic proteins were enriched in this set of GIT1-regulated phosphoproteins. We used the union of lists of biochemically purified pre-synaptic proteins[62] and post-synaptic proteins[30] as a reference list of ‘synaptic proteins’, which

totaled 1370 proteins, or ~6%, out of a total of 22032 protein-encoding genes in the mouse genome according to Gencode (http://www.gencodegenes.org/mouse_stats.html). Of these synaptic proteins, 1206, or ~14%, were present among the 8726 protein-expressing genes' products we detected as expressed in mouse hippocampus. The occurrence of synaptic phospho-proteins in our GIT1-regulated set by pure random chance would therefore be 10 (i.e. 14% of 73). In fact, we observed 27 synaptic protein phosphorylation states among the set of phospho-proteins regulated at least 2-fold by GIT1. This enrichment of synaptic phospho-proteins regulated by GIT1 was statistically significant (Figure 3A; $p < 0.0001$ by Chi-square test with Yates correction). Accordingly, GO cellular component enrichment analysis (using PANTHER) among GIT1-regulated hippocampal phospho-proteins (Figure 3B) showed that the vast majority of the enriched categories, as ranked by the degree of fold enrichment, involved V-type ATPases and synaptic components (see Supplemental Table 9 for a list of all enriched cellular component categories; the cell compartment specific subset of these categories visualized the in treemap in Figure 3B is listed in Supplemental Table 10). Indeed, the V-type ATPase categories may also be considered as synaptic components, as V-type ATPases function to facilitate loading of synaptic vesicles with neurotransmitters[82]. These data indicate that one of GIT1's primary roles in the hippocampus is to regulate levels of synaptic protein phosphorylation.

Inspection of the set of synaptic proteins with phosphorylation states regulated by GIT1 indicated that these proteins fell into the same functional categories as has been reported for GIT1-associated proteins in the brain[17]. Of synaptic phosphoproteins changed by more than 2-fold, 9 are involved in presynaptic vesicle functions, 10 are involved in post-synaptic density functions, and 16 regulate the cytoskeleton. For example, phospho-SEPT3 (serine 92) was downregulated by more than 70% by *GIT1* knockout. SEPT3 is known to be a phosphoprotein localized to presynaptic nerve terminals, and it appears to be involved in synaptic vesicle recycling[83]. Phosphorylation of serine 499 of the post-synaptic density scaffolding protein SHANK1 was upregulated more than 3.1-fold. DOCK10 phosphorylation at tyrosine 1980 was downregulated by nearly 58%. DOCK10 is a dendritic spine cytoskeleton regulator that acts through effects on CDC42, N-WASP, PAK3, and RAC1[84]. Phosphorylation of another neuronal cytoskeleton regulator, MACF1 (serine 7245), was downregulated by 56%. Both DOCK10 and MACF1 have been reported to regulate dendrite (or dendritic spine) and axon growth[84, 85]. Thus, GIT1 regulates the phosphorylation states of synaptic proteins associated with the functions of synaptic vesicles, the post-synaptic density, the neuronal cytoskeleton, and axon and dendrite growth.

To identify the protein networks with phosphorylation states dependent on the presence of GIT1 in an unbiased manner, we performed pathway enrichment analysis with the Reactome curated pathway database (www.reactome.org). This tool uses a set of user input seed proteins, in the present case identified in our unbiased proteomics experiment, to search a manually curated database covering protein-protein interactions across a wide swath of human molecular physiology and disease, and then generates error-corrected false discovery rate (FDR) values for pathway over-representation. Included in this database are brain pathways that are specific to neurons in general, specific types of neurons (defined by neurotransmitter type), and glia. Initially, we tested a seed set consisting of all phospho-proteins identified in control or GIT1-NKO hippocampi (6596 phospho-proteins, many of

which were phosphorylated at multiple sites; see Supplemental Table 3). No pathways were enriched in this 'total hippocampal phospho-proteome' seed set; all pathways had a FDR value > ~0.9. We next used a seed set consisting of all phospho-proteins regulated by more than 30% (up or down; 512 phospho-proteins; see Supplemental Table 7) by *GIT1* neural knockout. With this 'GIT1-regulated hippocampal phospho-proteome' seed set, four pathways had FDR values < 0.05 (Supplemental Table 8). The most statistically enriched pathway was 'Neuronal system', consistent with the notion that GIT1 regulates phospho-proteins in neurons, and indicating that the Reactome database is sufficiently annotated to detect organ-specific pathways. The other statistically significantly enriched pathways involved molecular interactions that connect and support synapses (e.g. neurexin-neuroligin interactions). A number of nominally significant pathways (FDR < 0.1) involved mechanisms of neurotransmission at synapses common to several neurotransmitter types, in particular including excitatory glutamatergic synapses. A growing body of genetic research implicates both neurexin-neuroligin interactions and excitatory glutamatergic synapses with cognition and neuropsychiatric disease[16, 86]. Thus, these unbiased Reactome-generated observations of statistically enriched pathways involving phospho-proteins regulated by GIT1 suggest that defects in GIT1 signal transduction functions at excitatory synapses may underlie pathology in neuropsychiatric diseases.

To further delineate GIT1's role in excitatory synapses, we examined levels of glutamate receptors in our hippocampal proteomics data. In these data (Supplemental Table 12), we detected NMDA receptors (GRIN2A, 2B, 2D, and 3A), AMPA receptors (GRIA1–3), kainate receptors (GRIK2, 3, and 5), and metabotropic glutamate receptors (GRM1–5, 7, and 8). Of these, only GRIA3 was affected by *GIT1* knockout by our statistical criteria (same direction of effect in all four replicate pairs; $p < 0.05$, see Materials and Methods for details), and it was downregulated. Loss of function mutations in GRIA3 can cause intellectual disability (Yuan et al., 2015). For comparison, we also looked at GABA receptors (type A—GABRA1–6; and type B—GABBR1–2) and found no statistically significant effect. We also performed western blotting analysis of several glutamate and GABA receptor proteins, utilizing hippocampal samples from a separate set of *GIT1*-NKO and control mice, to confirm these data. As controls, western blotting analysis of GIT1 and its tight binders ARHGEF6/7 showed the expected knockout and statistically significant downregulation, respectively (Supplemental Figure 5 and Supplemental Table 12). For the glutamate and GABA receptor proteins that we were able to test by western blotting, we found no statistically significant effects (Supplemental Table 12), consistent with our proteomics data. Interestingly, we also tested levels of the enzyme that synthesizes GABA (GAD1), and we found it to be statistically significantly downregulated (Supplemental Figure 5B). Downregulation of GAD1 was also caused by GIT1 loss of function variants found in schizophrenia patients (Kim et al., 2017), and we also saw a trend towards downregulation of GAD1 in our proteomics data that did not reach statistical significance (Supplemental Table 12). Lastly, several synaptic scaffolding proteins, such as PSD93/95, were unaffected by *GIT1* knockout (Supplemental Figure 5E). Thus, *GIT1* knockout produces specific deficits in the expression of two key proteins involved in glutamatergic and GABAergic synaptic transmission: the AMPA receptor GRIA3 and GAD1. These

observations are consistent with reports indicating that GIT1 regulates AMPA receptor targeting (Ko et al., 2003) and GABA levels (Kim et al., 2017).

Our observations of GIT1's importance for learning and memory (Figure 1) and its role in regulating synaptic protein phosphorylation raise the question of whether GIT1 regulates phospho-proteins known to play roles in learning-associated synaptic plasticity processes such as long-term potentiation (LTP) and/or long-term depression (LTD)[87]. Indeed, several proteins with phosphorylation states robustly regulated (> 2-fold) by GIT1 are known to participate in LTP and/or LTD. These proteins include ARHGEF6[88], PAK1[89], RIMS1[90], AKAP5[91, 92], STXBP1[93], MAP1A[94], SYT7[95], STMN1[96], NSMF[97], and CAMK2B[98]. Regulation of the phosphorylation states of any of these synaptic plasticity-associated proteins may underlie GIT1's role in learning and memory. We also utilized a proximity labeling 'Bio-ID' approach[49] to detect proteins that interact with GIT1 in neuronal cells (Supplemental Figure 4), and several GIT1-interacting proteins identified by this approach have been shown, in gene knockout studies, to play critical roles in hippocampal plasticity and/or cognition, including SCRIB[99], ACTR2/3[100], and AFDN[101]. Taken together, these data support the notion of GIT1 scaffolding protein-protein interactions and regulating kinase signaling cascades that underlie cognition.

Schizophrenia risk genes in GIT1-regulated synaptic phospho-protein networks

Having identified GIT1-regulated phospho-proteins at the synapse, we next asked whether any of these proteins have been associated with risk for schizophrenia. To address this question, we intersected the list of GIT1-regulated synaptic phospho-proteins (Supplemental Table 7) with schizophrenia risk genes identified in a study of common variation in schizophrenia patients[5]. This analysis revealed three GIT1-regulated synaptic phospho-proteins that have common variants that are associated with risk for schizophrenia: RIMS1, GRIN2A, and CNKSR2. Notably, GIT1 has been reported to directly interact with one of these proteins: CNKSR2[22]; we have been able to reproduce observation of this interaction using a co-immunoprecipitation assay in HEK293 cells (Supplemental Figure 2). The effect of GIT1 knockout on the phosphorylation status of these three proteins is shown in Figure 4A (black bars). Notably, two of these GIT1-regulated, schizophrenia-associated proteins (CNKSR2 and GRIN2A) are also associated with intellectual disability[23, 102]. We next constructed pre- and post-synaptic GIT1-schizophrenia risk gene interaction networks (Figure 4B and C) using GIT1 and RIMS1 (presynaptic), or GIT1 and CNKSR2 (postsynaptic) as starting nodes, and then adding interacting nodes from the sets of GIT1-regulated phospho-proteins (Supplemental Table 7) known to be expressed in those two synaptic compartments, particularly in excitatory glutamatergic synapses[30, 62], with interactions (edges) from the BioGRID protein interaction database (https://thebiogrid.org/). The effect of *GIT1* knockout on phosphorylation of a subset of these pre- and post-synaptic proteins is shown in Figure 4A (grey bars). Several proteins in these networks are known to be encoded by autism [103](Sanders et al., 2015) or developmental delay[104] risk genes (marked in Figure 4B) and it is possible that several more of the genes encoding these networks' proteins will be identified as schizophrenia risk genes in future studies as schizophrenia GWAS and sequencing sample sizes increase. Future work will be required

to determine how these phosphorylation changes affect the functioning of GIT1-regulated pre- and post-synaptic networks, and the behavioral consequences of the effects on these networks; however, the current literature contains some clues. For example, GIT1 knockout dramatically induces phosphorylation of CAMK2B at threonine 325, which is a residue in its actin-binding domain; this may allow CAMK2B to dissociate from actin during signaling events that induce synaptic plasticity and dendritic spine actin remodeling[105], suggesting that GIT1 may function to negatively regulate synaptic plasticity-associated dendritic remodeling through suppression of CAMK2B phosphorylation. In addition, mutation of several phosphorylated residues in GRIN2A to alanine, including GIT1-regulated S1291 and Y1292, caused deficits in Y-maze working memory[106] similar to the effect of GIT1 neural knockout observed here (Figure 1C). The identification of pre- and post-synaptic networks containing GIT1-regulated phospho-proteins, including schizophrenia and intellectual disability risk genes, clearly suggests the central role of GIT1-regulated proteins in a hot spot for neuropsychiatric disease pathology—the excitatory glutamatergic synapse.

Discussion

Building on recent efforts to elucidate the genetic architecture of neuropsychiatric diseases, the delineation of components, interactions, and signal transduction flow in key molecular networks and pathways that are disrupted in these diseases is a critical next step for the field. Here we study one such component with function and expression altering genetic variation in schizophrenia and neurodevelopmental disorders: the synaptic scaffolding and signaling protein GIT1. We utilize behavioral testing and phospho-proteomic analysis in mice with conditional neural-specific knockout of *GIT1* to identify aspects of cognition, as well as hippocampal phosphorylation signaling events that are regulated by GIT1. We find that *GIT1* neural knockout mice have cognitive deficits in associative memory recall and working memory, while social interaction, sensorimotor gating, and anxiety behaviors were normal. The impaired performance of *GIT1* neural-specific knockout mice in fear conditioning suggests that, in addition to primary cognitive deficits, these mice may also have aberrant amygdala-mediated emotional processing, as was also speculated to be the case in whole-body *GIT1* knockout mice[33]. Deficits in emotional processing have also been reported in schizophrenia patients[107–110]. As is also seen in whole-body *GIT1* knockout mice, *GIT1* neural-specific knockout mice have reduced cortical neuron dendritic spine density, suggesting reduced synaptic function. Our proteomic analyses indicate that GIT1 regulates phosphorylation states within networks of pre- and post-synaptic proteins. Excitingly, this includes a set of proteins within these synaptic networks that have been implicated as risk factors in genetic studies of schizophrenia and neurodevelopmental disorders. These data suggest that deficits in GIT1 functioning in synaptic networks may contribute to cognitive dysfunction in neuropsychiatric diseases.

Copy number variation at the *GIT1* locus, including both deletions and duplications, has been reported in patients with neurodevelopmental disorders[20]; these patients generally have developmental delay and intellectual disability. Hamdan and colleagues (2014) reported a *de novo* splice site variant in *GIT1* in a patient with intellectual disability. Here we identified cognitive deficits in a mouse model with complete nervous system-specific knockout of *GIT1*. Previous studies reporting associative learning deficits in

GIT1 knockout mice[33–36] utilized whole-body knockout, which produces post-natal cardiovascular dysfunction and lethality[33, 37]. In contrast, mice studied here with neural-specific *GIT1* knockout had normal post-natal survival. Consistent with whole-body knockout mice, neural-specific *GIT1* knockouts had an associative learning deficit in the fear conditioning test (Figure 1). In addition, we found that neural-specific *GIT1* knockout mice had a severe working memory deficit in the spontaneous alternation test (Figure 1). These findings suggest functional deficits in both the hippocampus and cortex, which are key brain regions involved in associative learning and working memory[51, 53]. Taken together with the observation that knockout of the GIT1-regulated kinase PAK3 causes deficits in hippocampal LTP and associative learning recall[111], these findings also point to cascades of phosphorylation-mediated signaling underlying learning and memory.

To begin to elucidate the molecular mechanism of GIT1's role in learning and memory, we performed phospho-proteomic analysis of GIT1-regulated signaling in the hippocampus. The set of hippocampal phospho-proteins regulated by GIT1 contained many synaptic proteins that fell within several functional categories: presynaptic vesicle trafficking, post-synaptic receptor clustering, and post-synaptic dendritic spine cytoskeleton regulation. Excitingly, several GIT1-regulated hippocampal phospho-proteins in these functional categories have common genetic variants associated with schizophrenia: RIMS1, GRIN2A, and CNKSR2. (The complete list of GIT1-regulated phospho-proteins that are schizophrenia GWAS genes is shown in Supplemental Table 11.) That these phosphorylation state-altering effects of GIT1 knockout were detectable is even more remarkable when considering that our samples consisted of whole hippocampus homogenate, containing a mixture of proteins from multiple cell types, which may have obscured some effects. Thus, these data link GIT1 to an apparent hotspot for schizophrenia pathology—the excitatory glutamatergic synapse.

GIT1 regulation of phosphorylation of the presynaptic vesicle trafficking protein PCLO is especially intriguing in light of the recently reported role of GIT1 in negatively regulating presynaptic vesicle release probability, possibly by regulating actin dynamics at the active zone[32]. PCLO also appears to negatively regulate synaptic vesicle exocytosis via effects on actin[112]. We hypothesize that GIT1-regulated phosphorylation of PCLO may facilitate PCLO's actions on the active zone actin cytoskeleton. This effect may be modulated by neuronal activity, as depolarization also regulates a subset of the GIT1-regulated phospho-sites in PCLO[113]. These will be important questions to address in future studies.

GIT1 regulation of phosphorylation of the schizophrenia-associated NMDA receptor subunit GRIN2A may play a role in the working memory deficit we observed in the spontaneous alternation test. Two GRIN2A phosphorylation sites that had decreased levels of phosphorylation in *GIT1*-NKO mice (serine 1291 and tyrosine 1292) may be required for performance of this task—Balu and colleagues[106] found that mice with these two residues mutated to alanine and phenylalanine, respectively, showed a deficit in the spontaneous alternation test.

In schizophrenia patients, several rare coding/splicing variants of *GIT1* have been identified[6–8]. Some of these variants impair GIT1 signaling via activation of PAK3 kinase[18]. To date, common variation at the *GIT1* locus has not been associated with risk

for schizophrenia[5]; however, as shown here, GIT1-regulated molecular networks include a number of genes at loci at which common variation has been associated with schizophrenia risk. To assess the effects of rare coding variants on GIT1-associated molecular networks, it will be necessary to study model systems expressing these variants, such as transgenic mice, or human induced pluripotent stem cell-derived neurons from patients with these coding variants. These studies are currently under way in our laboratory. Intriguingly, a putative GIT1 interacting protein identified here using the Bio-ID approach—AFDN (aka afadin/AF6)—is known to interact with a complex that promotes phosphorylation and activation of PAKs in dendritic spines (Xie et al., 2008). Although this interaction identified by Bio-ID will need future confirmation with orthogonal methods, we speculate that dysregulation of these interactions could underlie alterations of dendritic spine function observed in neuropsychiatric disease.

Supplementary Material

Refer to Web version on PubMed Central for supplementary material.

Acknowledgments

We thank members of the Stanley Center for Psychiatric Research and the Chemical Neurobiology Laboratory for helpful discussions and critical feedback. Dr. Guoping Feng is thanked for generously sharing GIT1 mice and for his critical feedback. This work was supported by funding from the Stanley Medical Research Institute, the National Institute of Mental Health (R01MH095088), and the Stuart & Suzanne Steele MGH Research Scholar Award (SJH).

References

[1]. Vissers LE, Gilissen C, Veltman JA. Genetic studies in intellectual disability and related disorders. Nat Rev Genet. 2016;17:9–18. [PubMed: 26503795]

[2]. McGrath J, Saha S, Chant D, Welham J. Schizophrenia: a concise overview of incidence, prevalence, and mortality. Epidemiol Rev. 2008;30:67–76. [PubMed: 18480098]

[3]. Kahn RS, Keefe RS. Schizophrenia is a cognitive illness: time for a change in focus. JAMA Psychiatry. 2013;70:1107–12. [PubMed: 23925787]

[4]. Tandon R, Gaebel W, Barch DM, Bustillo J, Gur RE, Heckers S, et al. Definition and description of schizophrenia in the DSM-5. Schizophr Res. 2013;150:3–10. [PubMed: 23800613]

[5]. Biological insights from 108 schizophrenia-associated genetic loci. Nature. 2014;511:421–7. [PubMed: 25056061]

[6]. Fromer M, Pocklington AJ, Kavanagh DH, Williams HJ, Dwyer S, Gormley P, et al. De novo mutations in schizophrenia implicate synaptic networks. Nature. 2014;506:179–84. [PubMed: 24463507]

[7]. Purcell SM, Moran JL, Fromer M, Ruderfer D, Solovieff N, Roussos P, et al. A polygenic burden of rare disruptive mutations in schizophrenia. Nature. 2014;506:185–90. [PubMed: 24463508]

[8]. Genovese G, Fromer M, Stahl EA, Ruderfer DM, Chambert K, Landen M, et al. Increased burden of ultra-rare protein-altering variants among 4,877 individuals with schizophrenia. Nat Neurosci. 2016;19:1433–41. [PubMed: 27694994]

[9]. Pardinas AF, Holmans P, Pocklington AJ, Escott-Price V, Ripke S, Carrera N, et al. Common schizophrenia alleles are enriched in mutation-intolerant genes and in regions under strong background selection. Nat Genet. 2018;50:381–9. [PubMed: 29483656]

[10]. Cristino AS, Williams SM, Hawi Z, An JY, Bellgrove MA, Schwartz CE, et al. Neurodevelopmental and neuropsychiatric disorders represent an interconnected molecular system. Mol Psychiatry. 2014;19:294–301. [PubMed: 23439483]

[11]. Hormozdiari F, Penn O, Borenstein E, Eichler EE. The discovery of integrated gene networks for autism and related disorders. Genome Res. 2015;25:142–54. [PubMed: 25378250]

[12]. Broek JAC, Lin Z, de Gruiter HM, van 't Spijker H, Haasdijk ED, Cox D, et al. . Synaptic vesicle dynamic changes in a model of fragile X. Mol Autism. 2016;7:17. [PubMed: 26933487]

[13]. Pechstein A, Shupliakov O, Haucke V. Intersectin 1: a versatile actor in the synaptic vesicle cycle. Biochem Soc Trans. 2010;38:181–6. [PubMed: 20074056]

[14]. Egbujo CN, Sinclair D, Hahn CG. Dysregulations of Synaptic Vesicle Trafficking in Schizophrenia. Curr Psychiatry Rep. 2016;18:77. [PubMed: 27371030]

[15]. Volk L, Chiu SL, Sharma K, Huganir RL. Glutamate synapses in human cognitive disorders. Annu Rev Neurosci. 2015;38:127–49. [PubMed: 25897873]

[16]. Hall J, Trent S, Thomas KL, O'Donovan MC, Owen MJ. Genetic risk for schizophrenia: convergence on synaptic pathways involved in plasticity. Biological psychiatry. 2015;77:52–8. [PubMed: 25152434]

[17]. Zhou W, Li X, Premont RT. Expanding functions of GIT Arf GTPase-activating proteins, PIX Rho guanine nucleotide exchange factors and GIT-PIX complexes. J Cell Sci. 2016;129:1963–74. [PubMed: 27182061]

[18]. Kim MJ, Biag J, Fass DM, Lewis MC, Zhang Q, Fleishman M, et al. Functional analysis of rare variants found in schizophrenia implicates a critical role for GIT1-PAK3 signaling in neuroplasticity. Mol Psychiatry. 2017;22:417–29. [PubMed: 27457813]

[19]. Datta D, Arion D, Corradi JP, Lewis DA. Altered expression of CDC42 signaling pathway components in cortical layer 3 pyramidal cells in schizophrenia. Biological psychiatry. 2015;78:775–85. [PubMed: 25981171]

[20]. Uddin M, Pellecchia G, Thiruvahindrapuram B, D'Abate L, Merico D, Chan A, et al. Indexing Effects of Copy Number Variation on Genes Involved in Developmental Delay. Sci Rep. 2016;6:28663. [PubMed: 27363808]

[21]. Lek M, Karczewski KJ, Minikel EV, Samocha KE, Banks E, Fennell T, et al. Analysis of protein-coding genetic variation in 60,706 humans. Nature. 2016;536:285–91. [PubMed: 27535533]

[22]. Lim J, Ritt DA, Zhou M, Morrison DK. The CNK2 scaffold interacts with vilse and modulates Rac cycling during spine morphogenesis in hippocampal neurons. Curr Biol. 2014;24:786–92. [PubMed: 24656827]

[23]. Houge G, Rasmussen IH, Hovland R. Loss-of-Function CNKSR2 Mutation Is a Likely Cause of Non-Syndromic X-Linked Intellectual Disability. Mol Syndromol. 2012;2:60–3. [PubMed: 22511892]

[24]. Ko J, Kim S, Valtschanoff JG, Shin H, Lee JR, Sheng M, et al. . Interaction between liprin-alpha and GIT1 is required for AMPA receptor targeting. The Journal of neuroscience : the official journal of the Society for Neuroscience. 2003;23:1667–77. [PubMed: 12629171]

[25]. Kutsche K, Yntema H, Brandt A, Jantke I, Nothwang HG, Orth U, et al. Mutations in ARHGEF6, encoding a guanine nucleotide exchange factor for Rho GTPases, in patients with X-linked mental retardation. Nat Genet. 2000;26:247–50. [PubMed: 11017088]

[26]. Bagrodia S, Bailey D, Lenard Z, Hart M, Guan JL, Premont RT, et al. A tyrosine-phosphorylated protein that binds to an important regulatory region on the cool family of p21-activated kinase-binding proteins. J Biol Chem. 1999;274:22393–400. [PubMed: 10428811]

[27]. Allen KM, Gleeson JG, Bagrodia S, Partington MW, MacMillan JC, Cerione RA, et al. PAK3 mutation in nonsyndromic X-linked mental retardation. Nat Genet. 1998;20:25–30. [PubMed: 9731525]

[28]. Zhang H, Webb DJ, Asmussen H, Horwitz AF. Synapse formation is regulated by the signaling adaptor GIT1. J Cell Biol. 2003;161:131–42. [PubMed: 12695502]

[29]. Zhang H, Webb DJ, Asmussen H, Niu S, Horwitz AF. A GIT1/PIX/Rac/PAK signaling module regulates spine morphogenesis and synapse formation through MLC. The Journal of neuroscience : the official journal of the Society for Neuroscience. 2005;25:3379–88. [PubMed: 15800193]

[30]. Collins MO, Husi H, Yu L, Brandon JM, Anderson CN, Blackstock WP, et al. Molecular characterization and comparison of the components and multiprotein complexes in the postsynaptic proteome. J Neurochem. 2006;97 Suppl 1:16–23. [PubMed: 16635246]

[31]. Kim S, Ko J, Shin H, Lee JR, Lim C, Han JH, et al. The GIT family of proteins forms multimers and associates with the presynaptic cytomatrix protein Piccolo. J Biol Chem. 2003;278:6291–300. [PubMed: 12473661]

[32]. Montesinos MS, Dong W, Goff K, Das B, Guerrero-Given D, Schmalzigaug R, et al. Presynaptic Deletion of GIT Proteins Results in Increased Synaptic Strength at a Mammalian Central Synapse. Neuron. 2015;88:918–25. [PubMed: 26637799]

[33]. Schmalzigaug R, Rodriguiz RM, Bonner PE, Davidson CE, Wetsel WC, Premont RT. Impaired fear response in mice lacking GIT1. Neurosci Lett. 2009;458:79–83. [PubMed: 19383529]

[34]. Won H, Mah W, Kim E, Kim JW, Hahm EK, Kim MH, et al. GIT1 is associated with ADHD in humans and ADHD-like behaviors in mice. Nat Med. 2011;17:566–72. [PubMed: 21499268]

[35]. Martyn AC, Toth K, Schmalzigaug R, Hedrick NG, Rodriguiz RM, Yasuda R, et al. . GIT1 regulates synaptic structural plasticity underlying learning. PloS one. 2018;13:e0194350.

[36]. Menon P, Deane R, Sagare A, Lane SM, Zarcone TJ, O'Dell MR, et al. . Impaired spine formation and learning in GPCR kinase 2 interacting protein-1 (GIT1) knockout mice. Brain Res. 2010;1317:218–26. [PubMed: 20043896]

[37]. Pang J, Hoefen R, Pryhuber GS, Wang J, Yin G, White RJ, et al. G-protein-coupled receptor kinase interacting protein-1 is required for pulmonary vascular development. Circulation. 2009;119:1524–32. [PubMed: 19273721]

[38]. Bates B, Rios M, Trumpp A, Chen C, Fan G, Bishop JM, et al. Neurotrophin-3 is required for proper cerebellar development. Nat Neurosci. 1999;2:115–7. [PubMed: 10195193]

[39]. Wolf A, Bauer B, Abner EL, Ashkenazy-Frolinger T, Hartz AM. A Comprehensive Behavioral Test Battery to Assess Learning and Memory in 129S6/Tg2576 Mice. PloS one. 2016;11:e0147733.

[40]. Clark RE, Zola SM, Squire LR. Impaired recognition memory in rats after damage to the hippocampus. The Journal of neuroscience : the official journal of the Society for Neuroscience. 2000;20:8853–60. [PubMed: 11102494]

[41]. Lotfipour S, Byun JS, Leach P, Fowler CD, Murphy NP, Kenny PJ, et al. . Targeted deletion of the mouse alpha2 nicotinic acetylcholine receptor subunit gene (Chrna2) potentiates nicotine-modulated behaviors. The Journal of neuroscience : the official journal of the Society for Neuroscience. 2013;33:7728–41. [PubMed: 23637165]

[42]. Hong ST, Mah W. A Critical Role of GIT1 in Vertebrate and Invertebrate Brain Development. Exp Neurobiol. 2015;24:8–16. [PubMed: 25792865]

[43]. Mertins P, Mani DR, Ruggles KV, Gillette MA, Clauser KR, Wang P, et al. Proteogenomics connects somatic mutations to signalling in breast cancer. Nature. 2016;534:55–62. [PubMed: 27251275]

[44]. Mundt F, Rajput S, Li S, Ruggles KV, Mooradian AD, Mertins P, et al. Mass spectrometry-based proteomics reveals potential roles of NEK9 and MAP2K4 in resistance to PI3K inhibitors in triple negative breast cancers. Cancer Res. 2018.

[45]. Elias JE, Gygi SP. Target-decoy search strategy for mass spectrometry-based proteomics. Methods Mol Biol. 2010;604:55–71. [PubMed: 20013364]

[46]. Nesvizhskii AI, Aebersold R. Interpretation of shotgun proteomic data: the protein inference problem. Mol Cell Proteomics. 2005;4:1419–40. [PubMed: 16009968]

[47]. Maere S, Heymans K, Kuiper M. BiNGO: a Cytoscape plugin to assess overrepresentation of gene ontology categories in biological networks. Bioinformatics. 2005;21:3448–9. [PubMed: 15972284]

[48]. Cheng C, Fass DM, Folz-Donahue K, MacDonald ME, Haggarty SJ. Highly Expandable Human iPS Cell-Derived Neural Progenitor Cells (NPC) and Neurons for Central Nervous System Disease Modeling and High-Throughput Screening. Current protocols in human genetics. 2017;92:21.8.1-.8.

[49]. Roux KJ, Kim DI, Burke B, May DG. BioID: A Screen for Protein-Protein Interactions. Current protocols in protein science. 2018;91:19.23.1–19.23.15.

[50]. Pang J, Yan C, Natarajan K, Cavet ME, Massett MP, Yin G, et al. . GIT1 mediates HDAC5 activation by angiotensin II in vascular smooth muscle cells. Arterioscler Thromb Vasc Biol. 2008;28:892–8. [PubMed: 18292392]

[51]. Kim JJ, Fanselow MS Modality-specific retrograde amnesia of fear. Science. 1992;256:675–7. [PubMed: 1585183]

[52]. Muller J, Corodimas KP, Fridel Z, LeDoux JE Functional inactivation of the lateral and basal nuclei of the amygdala by muscimol infusion prevents fear conditioning to an explicit conditioned stimulus and to contextual stimuli. Behav Neurosci. 1997;111:683–91. [PubMed: 9267646]

[53]. Lalonde R The neurobiological basis of spontaneous alternation. Neurosci Biobehav Rev. 2002;26:91–104. [PubMed: 11835987]

[54]. Dudchenko PA. An overview of the tasks used to test working memory in rodents. Neurosci Biobehav Rev. 2004;28:699–709. [PubMed: 15555679]

[55]. Silverman JL, Yang M, Lord C, Crawley JN. Behavioural phenotyping assays for mouse models of autism. Nature reviews Neuroscience. 2010;11:490–502. [PubMed: 20559336]

[56]. Braff D, Stone C, Callaway E, Geyer M, Glick I, Bali L. Prestimulus effects on human startle reflex in normals and schizophrenics. Psychophysiology. 1978;15:339–43. [PubMed: 693742]

[57]. Jordi E, Heiman M, Marion-Poll L, Guermonprez P, Cheng SK, Nairn AC, et al. Differential effects of cocaine on histone posttranslational modifications in identified populations of striatal neurons. Proc Natl Acad Sci U S A. 2013;110:9511–6. [PubMed: 23690581]

[58]. Vizi ES, Kiss JP. Neurochemistry and pharmacology of the major hippocampal transmitter systems: synaptic and nonsynaptic interactions. Hippocampus. 1998;8:566–607. [PubMed: 9882017]

[59]. Gonzalez-Burgos I, Feria-Velasco A. Serotonin/dopamine interaction in memory formation. Prog Brain Res. 2008;172:603–23. [PubMed: 18772052]

[60]. Harrison PJ. The hippocampus in schizophrenia: a review of the neuropathological evidence and its pathophysiological implications. Psychopharmacology (Berl). 2004;174:151–62. [PubMed: 15205886]

[61]. Woolfrey KM, Dell'Acqua ML. Coordination of Protein Phosphorylation and Dephosphorylation in Synaptic Plasticity. J Biol Chem. 2015;290:28604–12. [PubMed: 26453308]

[62]. Boyken J, Gronborg M, Riedel D, Urlaub H, Jahn R, Chua JJ. Molecular profiling of synaptic vesicle docking sites reveals novel proteins but few differences between glutamatergic and GABAergic synapses. Neuron. 2013;78:285–97. [PubMed: 23622064]

[63]. Zhao ZS, Manser E, Loo TH, Lim L. Coupling of PAK-interacting exchange factor PIX to GIT1 promotes focal complex disassembly. Mol Cell Biol. 2000;20:6354–63. [PubMed: 10938112]

[64]. Hsu RM, Tsai MH, Hsieh YJ, Lyu PC, Yu JS. Identification of MYO18A as a novel interacting partner of the PAK2/betaPIX/GIT1 complex and its potential function in modulating epithelial cell migration. Mol Biol Cell. 2010;21:287–301. [PubMed: 19923322]

[65]. Shin H, Wyszynski M, Huh KH, Valtschanoff JG, Lee JR, Ko J, et al. Association of the kinesin motor KIF1A with the multimodular protein liprin-alpha. J Biol Chem. 2003;278:11393–401. [PubMed: 12522103]

[66]. Frese S, Schubert WD, Findeis AC, Marquardt T, Roske YS, Stradal TE, et al. The phosphotyrosine peptide binding specificity of Nck1 and Nck2 Src homology 2 domains. J Biol Chem. 2006;281:18236–45. [PubMed: 16636066]

[67]. Ko J, Na M, Kim S, Lee JR, Kim E. Interaction of the ERC family of RIM-binding proteins with the liprin-alpha family of multidomain proteins. J Biol Chem. 2003;278:42377–85. [PubMed: 12923177]

[68]. Park E, Na M, Choi J, Kim S, Lee JR, Yoon J, et al. The Shank family of postsynaptic density proteins interacts with and promotes synaptic accumulation of the beta PIX guanine nucleotide exchange factor for Rac1 and Cdc42. J Biol Chem. 2003;278:19220–9. [PubMed: 12626503]

[69]. Martin HG, Henley JM, Meyer G. Novel putative targets of N-ethylmaleimide sensitive fusion protein (NSF) and alpha/beta soluble NSF attachment proteins (SNAPs) include the Pak-binding nucleotide exchange factor betaPIX. J Cell Biochem. 2006;99:1203–15. [PubMed: 16795052]

[70]. Fu CA, Shen M, Huang BC, Lasaga J, Payan DG, Luo. TNIK, a novel member of the germinal center kinase family that activates the c-Jun N-terminal kinase pathway and regulates the cytoskeleton. J Biol Chem. 1999;274:30729–37. [PubMed: 10521462]

[71]. Wang Q, Amato SP, Rubitski DM, Hayward MM, Kormos BL, Verhoest PR, et al. Identification of Phosphorylation Consensus Sequences and Endogenous Neuronal Substrates of the Psychiatric Risk Kinase TNIK. J Pharmacol Exp Ther. 2016;356:410–23. [PubMed: 26645429]

[72]. Yin G, Hasendeler J, Yan C, Berk BC. GIT1 functions as a scaffold for MEK1-extracellular signal-regulated kinase 1 and 2 activation by angiotensin II and epidermal growth factor. Mol Cell Biol. 2004;24:875–85. [PubMed: 14701758]

[73]. Yin G, Zheng Q, Yan C, Berk BC. GIT1 is a scaffold for ERK1/2 activation in focal adhesions. J Biol Chem. 2005;280:27705–12. [PubMed: 15923189]

[74]. Zhang N, Cai W, Yin G, Nagel DJ, Berk BC. GIT1 is a novel MEK1-ERK1/2 scaffold that localizes to focal adhesions. Cell Biol Int. 2009;34:41–7. [PubMed: 19947948]

[75]. Versele M, Thorner J. Septin collar formation in budding yeast requires GTP binding and direct phosphorylation by the PAK, Cla4. J Cell Biol. 2004;164:701–15. [PubMed: 14993234]

[76]. Wittmann T, Bokoch GM, Waterman-Storer CM. Regulation of microtubule destabilizing activity of Op18/stathmin downstream of Rac1. J Biol Chem. 2004;279:6196–203. [PubMed: 14645234]

[77]. Aslan JE, Baker SM, Loren CP, Haley KM, Itakura A, Pang J, et al. The PAK system links Rho GTPase signaling to thrombin-mediated platelet activation. Am J Physiol Cell Physiol. 2013;305:C519–28. [PubMed: 23784547]

[78]. Shin EY, Shim ES, Lee CS, Kim HK, Kim EG. Phosphorylation of RhoGDI1 by p21-activated kinase 2 mediates basic fibroblast growth factor-stimulated neurite outgrowth in PC12 cells. Biochem Biophys Res Commun. 2009;379:384–9. [PubMed: 19103160]

[79]. Vadlamudi RK, Manavathi B, Singh RR, Nguyen D, Li F, Kumar R. An essential role of Pak1 phosphorylation of SHARP in Notch signaling. Oncogene. 2005;24:4591–6. [PubMed: 15824732]

[80]. Rennefahrt UE, Deacon SW, Parker SA, Devarajan K, Beeser A, Chernoff J, et al. Specificity profiling of Pak kinases allows identification of novel phosphorylation sites. J Biol Chem. 2007;282:15667–78. [PubMed: 17392278]

[81]. Veeranna Amin ND, Ahn NG, Jaffe H, Winters CA, Grant P, et al. Mitogen-activated protein kinases (Erk1,2) phosphorylate Lys-Ser-Pro (KSP) repeats in neurofilament proteins NF-H and NF-M. The Journal of neuroscience : the official journal of the Society for Neuroscience. 1998;18:4008–21. [PubMed: 9592082]

[82]. Edwards RH. The neurotransmitter cycle and quantal size. Neuron. 2007;55:835–58. [PubMed: 17880890]

[83]. Xue J, Tsang CW, Gai WP, Malladi CS, Trimble WS, Rostas JA, et al. Septin 3 (G-septin) is a developmentally regulated phosphoprotein enriched in presynaptic nerve terminals. J Neurochem. 2004;91:579–90. [PubMed: 15485489]

[84]. Jaudon F, Raynaud F, Wehrle R, Bellanger JM, Doulazmi M, Vodjdani G, et al. The RhoGEF DOCK10 is essential for dendritic spine morphogenesis. Mol Biol Cell. 2015;26:2112–27. [PubMed: 25851601]

[85]. Ka M, Kim WY. Microtubule-Actin Crosslinking Factor 1 Is Required for Dendritic Arborization and Axon Outgrowth in the Developing Brain. Mol Neurobiol. 2016;53:6018–32. [PubMed: 26526844]

[86]. Doherty JL, O'Donovan MC, Owen MJ. Recent genomic advances in schizophrenia. Clin Genet. 2012;81:103–9. [PubMed: 21895634]

[87]. Nabavi S, Fox R, Proulx CD, Lin JY, Tsien RY, Malinow R. Engineering a memory with LTD and LTP. Nature. 2014;511:348–52. [PubMed: 24896183]

[88]. Ramakers GJ, Wolfer D, Rosenberger G, Kuchenbecker K, Kreienkamp HJ, Prange-Kiel J, et al. Dysregulation of Rho GTPases in the alphaPix/Arhgef6 mouse model of X-linked intellectual disability is paralleled by impaired structural and synaptic plasticity and cognitive deficits. Human molecular genetics. 2012;21:268–86. [PubMed: 21989057]

[89]. Asrar S, Meng Y, Zhou Z, Todorovski Z, Huang WW, Jia Z. Regulation of hippocampal long-term potentiation by p21-activated protein kinase 1 (PAK1). Neuropharmacology. 2009;56:73–80.

[90]. Castillo PE, Schoch S, Schmitz F, Sudhof TC, Malenka RC. RIM1alpha is required for presynaptic long-term potentiation. Nature. 2002;415:327–30. [PubMed: 11797010]

[91]. Diering GH, Gustina AS, Huganir RL. PKA-GluA1 coupling via AKAP5 controls AMPA receptor phosphorylation and cell-surface targeting during bidirectional homeostatic plasticity. Neuron. 2014;84:790–805. [PubMed: 25451194]

[92]. Sanderson JL, Gorski JA, Dell'Acqua ML. NMDA Receptor-Dependent LTD Requires Transient Synaptic Incorporation of Ca(2)(+)-Permeable AMPARs Mediated by AKAP150-Anchored PKA and Calcineurin. Neuron. 2016;89:1000–15. [PubMed: 26938443]

[93]. Orock A, Logan S, Deak F. Munc18–1 haploinsufficiency impairs learning and memory by reduced synaptic vesicular release in a model of Ohtahara syndrome. Molecular and cellular neurosciences. 2018;88:33–42. [PubMed: 29217410]

[94]. Takei Y, Kikkawa YS, Atapour N, Hensch TK, Hirokawa N. Defects in Synaptic Plasticity, Reduced NMDA-Receptor Transport, and Instability of Postsynaptic Density Proteins in Mice Lacking Microtubule-Associated Protein 1A. The Journal of neuroscience : the official journal of the Society for Neuroscience. 2015;35:15539–54. [PubMed: 26609151]

[95]. Wu D, Bacaj T, Morishita W, Goswami D, Arendt KL, Xu W, et al. Postsynaptic synaptotagmins mediate AMPA receptor exocytosis during LTP. Nature. 2017;544:316–21. [PubMed: 28355182]

[96]. Shumyatsky GP, Malleret G, Shin RM, Takizawa S, Tully K, Tsvetkov E, et al. stathmin, a gene enriched in the amygdala, controls both learned and innate fear. Cell. 2005;123:697–709. [PubMed: 16286011]

[97]. Spilker C, Nullmeier S, Grochowska KM, Schumacher A, Butnaru I, Macharadze T, et al. A Jacob/Nsmf Gene Knockout Results in Hippocampal Dysplasia and Impaired BDNF Signaling in Dendritogenesis. PLoS genetics. 2016;12:e1005907.

[98]. Lisman J, Yasuda R, Raghavachari S. Mechanisms of CaMKII action in long-term potentiation. Nature reviews Neuroscience. 2012;13:169–82. [PubMed: 22334212]

[99]. Hilal ML, Moreau MM, Racca C, Pinheiro VL, Piguel NH, Santoni MJ, et al. Activity-Dependent Neuroplasticity Induced by an Enriched Environment Reverses Cognitive Deficits in Scribble Deficient Mouse. Cerebral cortex (New York, NY : 1991). 2017;27:5635–51.

[100]. Kim IH, Racz B, Wang H, Burianek L, Weinberg R, Yasuda R, et al. Disruption of Arp2/3 results in asymmetric structural plasticity of dendritic spines and progressive synaptic and behavioral abnormalities. The Journal of neuroscience : the official journal of the Society for Neuroscience. 2013;33:6081–92. [PubMed: 23554489]

[101]. Beaudoin GM, 3rd, Schofield CM, Nuwal T, Zang K, Ullian EM, Huang B, et al. Afadin, a Ras/Rap effector that controls cadherin function, promotes spine and excitatory synapse density in the hippocampus. The Journal of neuroscience : the official journal of the Society for Neuroscience. 2012;32:99–110. [PubMed: 22219273]

[102]. Endele S, Rosenberger G, Geider K, Popp B, Tamer C, Stefanova I, et al. Mutations in GRIN2A and GRIN2B encoding regulatory subunits of NMDA receptors cause variable neurodevelopmental phenotypes. Nat Genet. 2010;42:1021–6. [PubMed: 20890276]

[103]. Sanders SJ, He X, Willsey AJ, Ercan-Sencicek AG, Samocha KE, Cicek AE, et al. . Insights into Autism Spectrum Disorder Genomic Architecture and Biology from 71 Risk Loci. Neuron. 2015;87:1215–33. [PubMed: 26402605]

[104]. Prevalence and architecture of de novo mutations in developmental disorders. Nature. 2017;542:433–8. [PubMed: 28135719]

[105]. Kim K, Lakhanpal G, Lu HE, Khan M, Suzuki A, Hayashi MK, et al. A Temporary Gating of Actin Remodeling during Synaptic Plasticity Consists of the Interplay between the Kinase and Structural Functions of CaMKII. Neuron. 2015;87:813–26. [PubMed: 26291163]

[106]. Balu D, Larson JR, Schmidt JV, Wirtshafter D, Yevtodiyenko A, Leonard JP. Behavioral and physiological characterization of PKC-dependent phosphorylation in the Grin2aPKC mouse. Brain Res. 2016;1646:315–26. [PubMed: 27317637]

[107]. Aleman A, Kahn RS. Strange feelings: do amygdala abnormalities dysregulate the emotional brain in schizophrenia? Progress in neurobiology. 2005;77:283–98. [PubMed: 16352388]

[108]. Holt DJ, Lebron-Milad K, Milad MR, Rauch SL, Pitman RK, Orr SP, et al. Extinction memory is impaired in schizophrenia. Biological psychiatry. 2009;65:455–63. [PubMed: 18986648]

[109]. Pinkham AE, Liu P, Lu H, Kriegsman M, Simpson C, Tamminga C. Amygdala Hyperactivity at Rest in Paranoid Individuals With Schizophrenia. The American journal of psychiatry. 2015;172:784–92. [PubMed: 25815418]

110. Potvin S, Tikasz A, Mendrek A Emotionally Neutral Stimuli Are Not Neutral in Schizophrenia: A Mini Review of Functional Neuroimaging Studies. Frontiers in psychiatry. 2016;7:115. [PubMed: 27445871]

111. Meng J, Meng Y, Hanna A, Janus C, Jia Z Abnormal long-lasting synaptic plasticity and cognition in mice lacking the mental retardation gene Pak3. The Journal of neuroscience : the official journal of the Society for Neuroscience. 2005;25:6641–50. [PubMed: 16014725]

112. Waites CL, Leal-Ortiz SA, Andlauer TF, Sigrist SJ, Garner CC Piccolo regulates the dynamic assembly of presynaptic F-actin. The Journal of neuroscience : the official journal of the Society for Neuroscience. 2011;31:14250–63. [PubMed: 21976510]

113. Kohansal-Nodehi M, Chua JJ, Urlaub H, Jahn R, Czernik D Analysis of protein phosphorylation in nerve terminal reveals extensive changes in active zone proteins upon exocytosis. Elife. 2016;5.

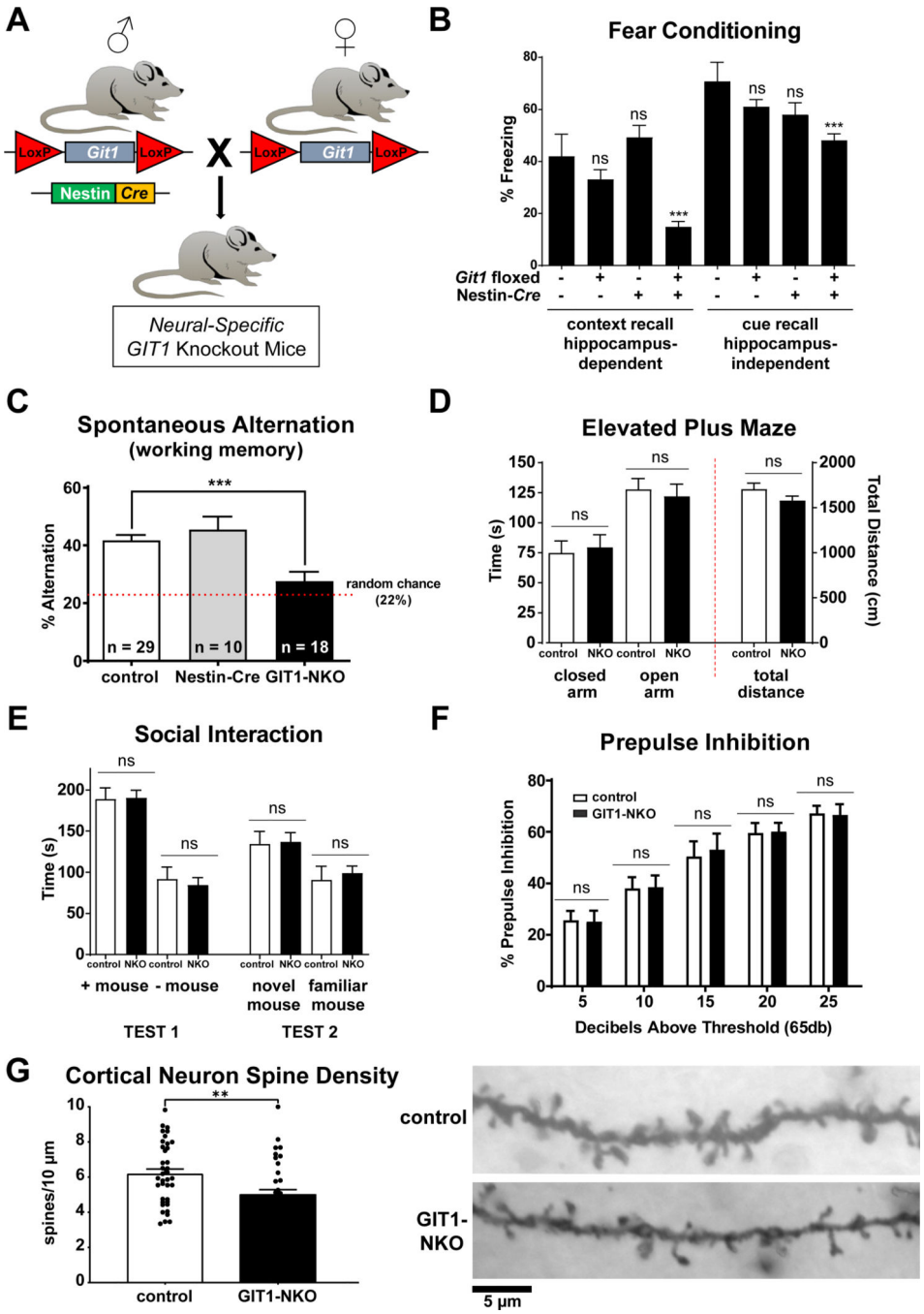

Figure 1. Cognitive deficits observed in *GIT1*-NKO mice tested in a battery of behavioral paradigms.

(A) *GIT1*-NKO mice were bred by crossing males carrying the Nestin-Cre transgene that is expressed specifically in neural tissues, with females homozygous for floxed *GIT1* allele (see Supplementary Figure 1), resulting in neural-specific *GIT1* knockout. **(B)** Context and cued fear conditioning tests. N = 8 ($GIT1^{+/+}$/Nestin-Cre^{-} control), 20 ($GIT1^{flox/flox}$/Nestin-Cre^{-} control), and 18 ($GIT1^{flox/flox}$/Nestin-Cre^{+} knockout). *** = $p < 0.001$; ns = not significant; one-way ANOVA followed by multiple comparison tests versus controls

with Sidak correction; bar graph displays means ± SEM. Variance across groups was not statistically significantly different by the Brown-Forsythe test, and all groups passed the D'Agostino & Pearson normality test ($\alpha = 0.05$). **(C)** T-maze spontaneous alternation test. Alternation was measured as the percentage of sets of three consecutive arm entries all occurring in non-previously visited arms over a 5 minute test period. N = 29 ($GIT1^{flox/flox}$/Nestin-Cre^{-} control), 10 ($GIT1^{+/+}$/Nestin-Cre^{+} control), and 18 ($GIT1^{flox/flox}$/Nestin-Cre^{+} knockout). *** = $p < 0.001$; ns = not significant; one-way ANOVA followed by multiple comparison tests versus control with Dunnett correction; bar graph displays means ± SEM. Variance across groups was not statistically significantly different by the Brown-Forsythe test, and all groups passed the Kolmogorov-Smirnov normality test ($\alpha = 0.05$). **(D)** Elevated plus maze test. N = 20 ($GIT1^{+/+}$/Nestin-Cre^{-} control), and 17 ($GIT1^{flox/flox}$/Nestin-Cre^{+} knockout). ns = not significant, two-tailed t-tests; bar graph displays means ± SEM. Variance across groups was not statistically significantly different by F test. **(E)** Social interaction test. N = 8 ($GIT1^{+/+}$/Nestin-Cre^{-} control), and 8 ($GIT1^{flox/flox}$/Nestin-Cre^{+} knockout). ns = not significant, two-tailed t-tests; bar graph displays means ± SEM. Variance across groups was not statistically significantly different by F test. **(F)** Prepulse inhibition test. N = 9 ($GIT1^{+/+}$/Nestin-Cre^{-} control), and 10 ($GIT1^{flox/flox}$/Nestin-Cre^{+} knockout). ns = not significant, two-way ANOVA; bar graph displays means ± SEM. (**G**) Cortical neuron dendritic spine density in WT and GIT1-NKO mice. Representative images of dendrite fragments with spines stained with the Golgi-Cox method are shown on right. N = 4 ($GIT1^{+/+}$/Nestin-Cre^{-} control), and 4 ($GIT1^{flox/flox}$/Nestin-Cre^{+} knockout); 8–10 dendrite fragment images were analyzed per animal. Bar graph displays means ± SEM, along with individual data points as small circles, and statistical p value was calculated using a two-tailed t-test; ** = $p < 0.01$. Variance across groups was not statistically significantly different by F test.

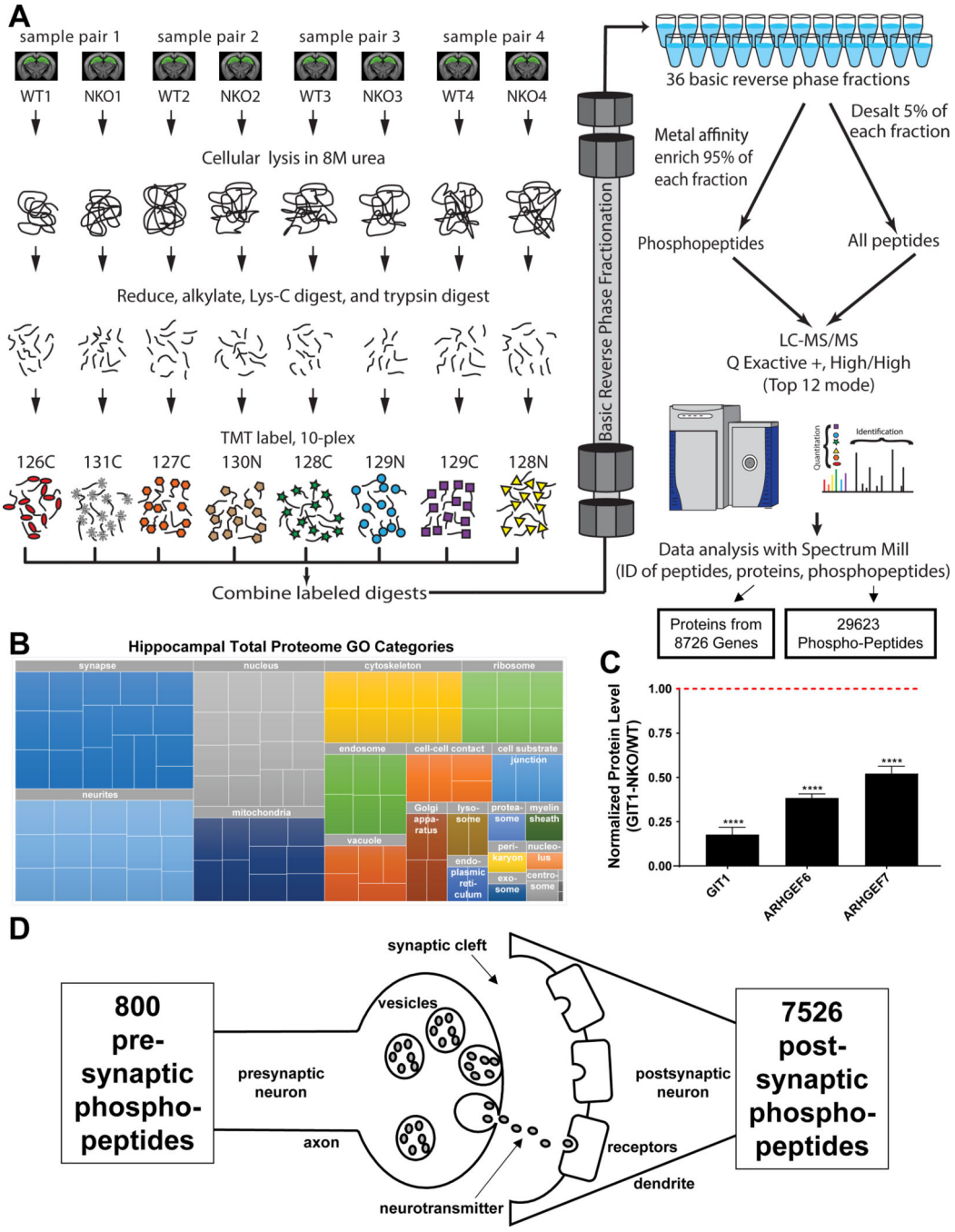

Figure 2. Global functional and synaptic analyses of mouse hippocampal proteome and phospho-proteome.

(A) Pipeline for discovery-based proteomic and phospho-proteomic profiling. Protein from dissected hippocampal (green region on coronal brain view) sample pairs was extracted with 8M urea and digested with LysC/trypsin. Peptides from each sample were labeled with chemical mass tag reagents for relative quantification; the 10-plex TMT labeling method is illustrated. Following labeling, peptides were combined and fractionated by basic reversed-phase (bRP) chromatography to decrease sample complexity and increase the dynamic range

of detection. The global proteome of each plex was measured with 24 bRP fractions using 60 h (24× 2.5 h runs) of measurement time on a Thermo Q Exactive Plus instrument. For phospho-proteome analysis, phosphorylated peptides were enriched with immobilized metal affinity chromatography (IMAC) and injected as 12 LC-MS/MS runs requiring 30 h assay time per plex. **(B)** Treemap of enriched GO cellular component categories in the set of all proteins detected in the mouse hippocampus. Branches are shown as distinct colored areas with branch names in white text; leaves are boxes within each branch; for a complete list of leaf names see. Supplemental Table 2. Leaf size corresponds to fold-enrichment values for each GO category. **(C)** Quantitated proteomic data indicating changes induced by *GIT1* neural knockout in the hippocampal levels of GIT1 and ARHGEF6/7. **** = $p < 0.0001$, unpaired t-tests; bar graph displays means ± SEM. Red dashed line indicates normalized level of protein in control hippocampi. **(D)** Diagram of a synapse indicating the number of phospho-peptides that we detected in mouse hippocampus that occur in proteins identified in published lists of pre- and post-synaptic proteins[30, 62].

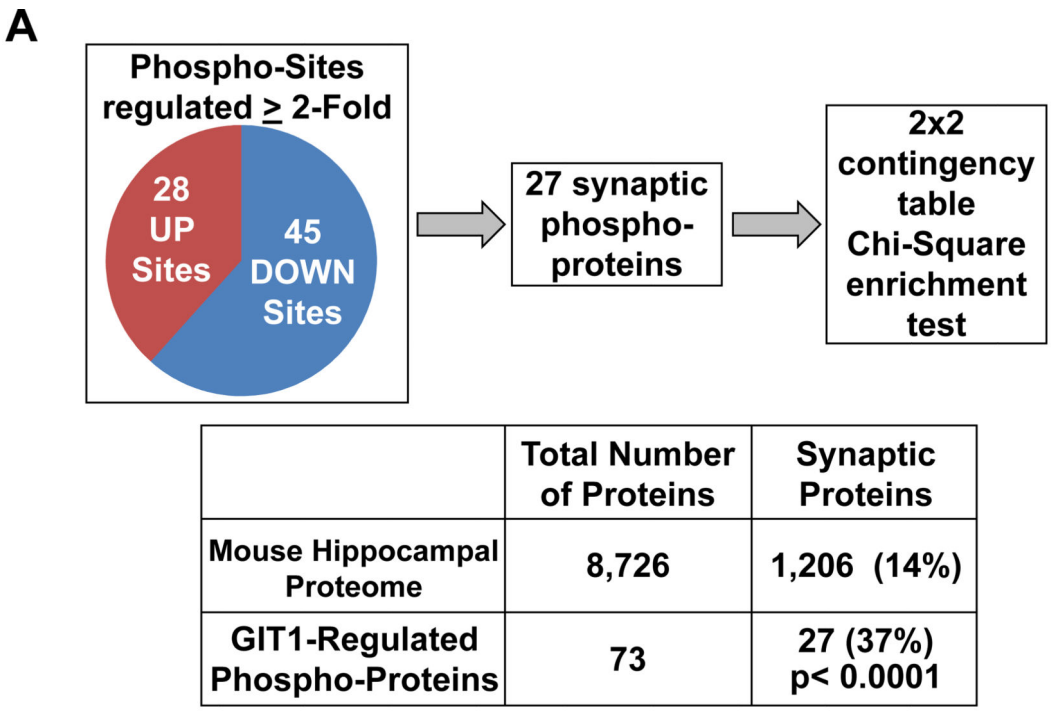

	Total Number of Proteins	Synaptic Proteins
Mouse Hippocampal Proteome	8,726	1,206 (14%)
GIT1-Regulated Phospho-Proteins	73	27 (37%) p< 0.0001

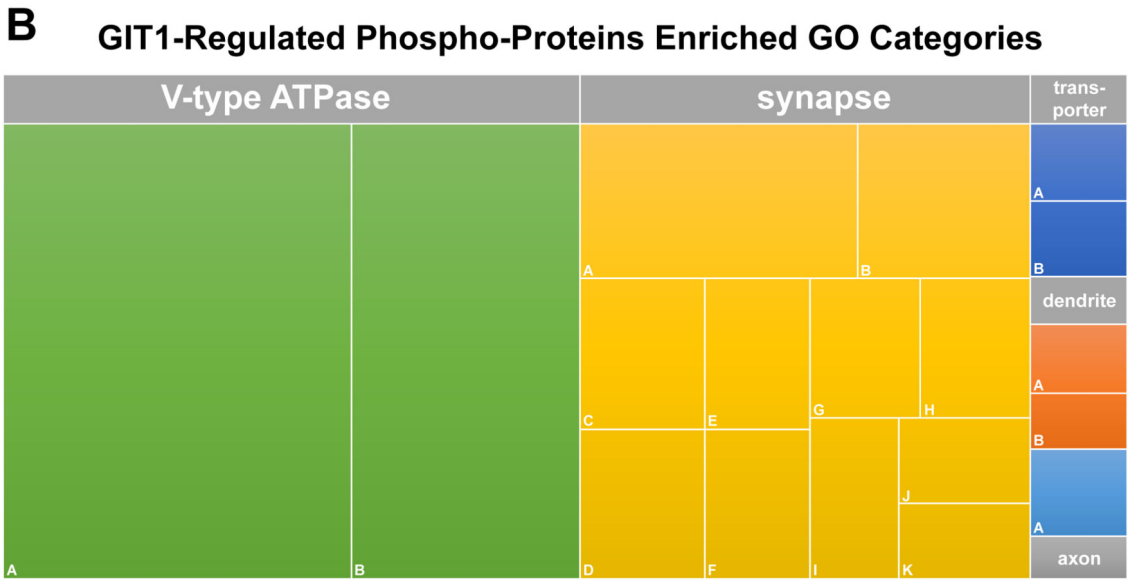

Figure 3. Enrichment of synaptic proteins in the set of hippocampal phospho-proteins regulated by GIT1.

(A) Statistical 2 X 2 contingency table Chi-square test of enrichment of synaptic proteins in the set of phospho-proteins robustly regulated (> 2-fold) by *GIT1* neural knockout. Synaptic proteins were defined as the union of the presynaptic and postsynaptic proteins identified[62] and https://www.genes2cognition.org/. **(B)** Treemap of GO cellular component categories enriched in the set of GIT1-regulated phospho-proteins detected in mouse hippocampus. Branches are shown as distinct colored areas with branch names

in white text; leaves are boxes within each branch; for a complete list of leaf names see Supplemental Table 10. Leaf size corresponds to fold-enrichment values for each GO category.

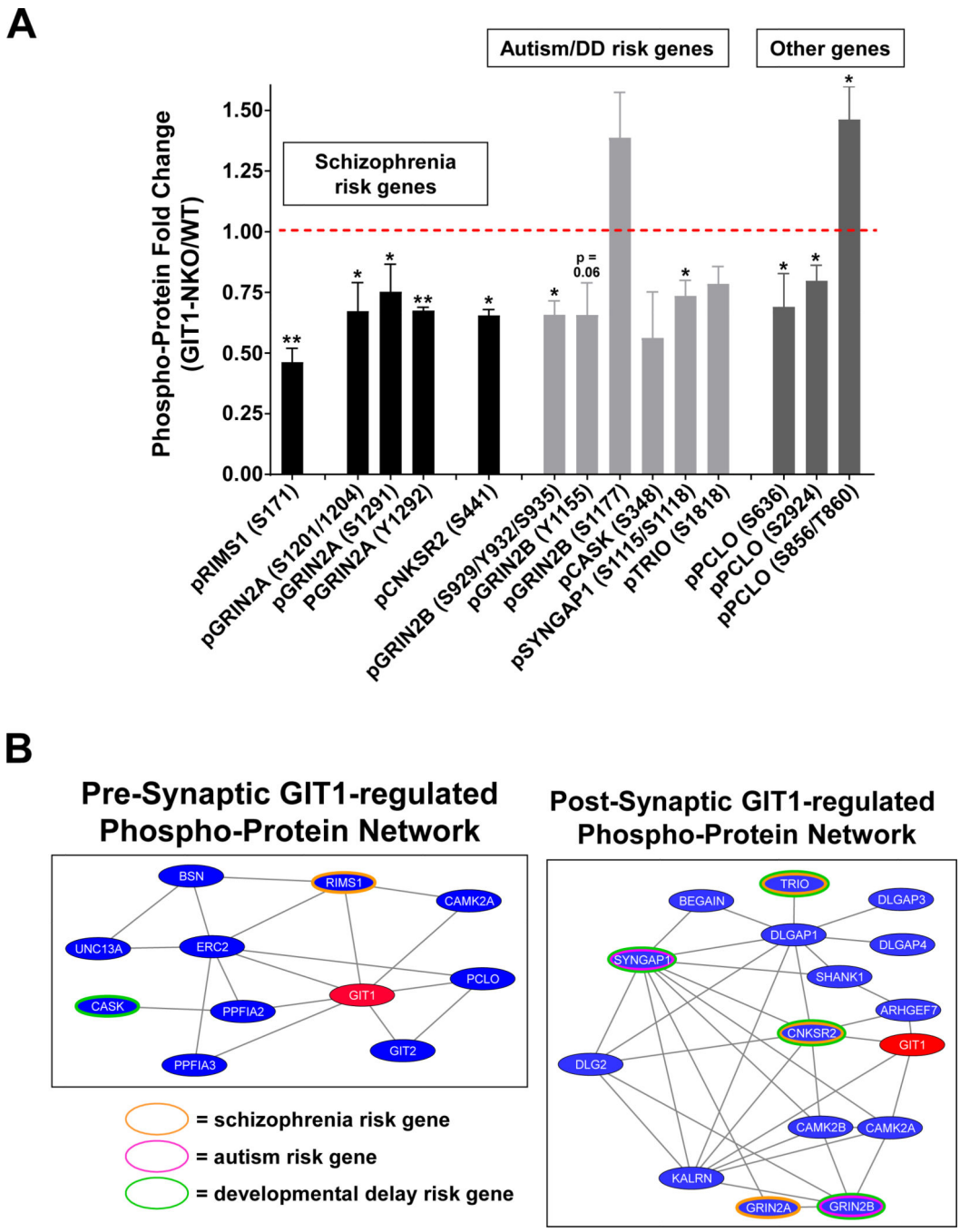

Figure 4. GIT1-regulated synaptic phosphorylation signaling events within a network of neuropsychiatric risk genes

(A) Effect of *GIT1* knockout on phosphorylation of several schizophrenia/autism/developmental delay risk gene proteins and a related presynaptic protein. * = $p < 0.05$; ** = $p < 0.01$; p values output by Spectrum Mill for the indicated phospho-protein sites; bar graph displays means ± SEM. **(B)** GIT1-regulated synaptic phospho-protein networks affected in neuropsychiatric diseases. Pre- and post-synaptic GIT1-neuropsychiatric disease risk gene phospho-protein interaction networks were constructed using interacting nodes from the

sets of GIT1-regulated phospho-proteins expressed in those two synaptic compartments identified in the BioGRID protein interaction database (https://thebiogrid.org/).